

AD-A269 114

2

NUWC-NPT Technical Report 10,200
28 May 1993



A Constrained Fuzzy Controller for Beam Rider Guidance

A. F. Bessacini
R. F. Pinkos
Combat Control Systems Department



DTIC
ELECTE
SEP 09 1993
S E D

Naval Undersea Warfare Center Division
Newport, Rhode Island

93-20918



3600 J

Approved for public release; distribution is unlimited.

9 3 0 0 8 1 0 2

PREFACE

This report was performed under the NUWC Bid and Proposal (B&P) Program. The B&P Program provides funding for preliminary, conceptual, and technical work necessary for the generation of complete and comprehensive proposals for direct-funded work.

The technical reviewer for this report was P. R. Kersten (Code 2211)

Reviewed and Approved: 28 May 1993



**P. A. La Brecque
Head, Combat Control Systems Department**

Accession For	
NTIS CRA&I	<input checked="" type="checkbox"/>
DTIC TAB	<input type="checkbox"/>
Unannounced	<input type="checkbox"/>
Justification	
By	
Distribution /	
Availability Codes	
Dist	Avail and/or Special
A-1	

DTIC QUALITY INSURED

REPORT DOCUMENTATION PAGE

Form Approved
OMB No. 0704-0188

Public reporting burden for this collection of information is estimated to average 1 hour per response, including the time for reviewing instructions, searching existing data sources, gathering and maintaining the data needed, and completing and reviewing the collection of information. Send comments regarding this burden estimate or any other aspect of this collection of information, including suggestions for reducing this burden, to Washington Headquarters Services, Directorate for Information Operations and Reports, 1215 Jefferson Davis Highway, Suite 1204, Arlington, VA 22202-4302, and to the Office of Management and Budget, Paperwork Reduction Project (0704-0188), Washington, DC 20503.

1. AGENCY USE ONLY (Leave blank)		2. REPORT DATE 28 May 1993	3. REPORT TYPE AND DATES COVERED Final	
4. TITLE AND SUBTITLE A Constrained Fuzzy Controller for Beam Rider Guidance			5. FUNDING NUMBERS	
6. AUTHOR(S) A. F. Bessacini R. F. Pinkos				
7. PERFORMING ORGANIZATION NAME(S) AND ADDRESS(ES) Naval Undersea Warfare Center Division Newport, Rhode Island 02841-1708			8. PERFORMING ORGANIZATION REPORT NUMBER TR 10,200	
9. SPONSORING/MONITORING AGENCY NAME(S) AND ADDRESS(ES)			10. SPONSORING/MONITORING AGENCY REPORT NUMBER	
11. SUPPLEMENTARY NOTES				
12a. DISTRIBUTION/AVAILABILITY STATEMENT Approved for public release; distribution is unlimited.			12b. DISTRIBUTION CODE	
13. ABSTRACT (Maximum 200 words) Fuzzy set theory was used to formulate a control system for beam rider guidance of a vehicle launched from a moving platform against an evasive contact. Control of the vehicle entails use of a time-varying data input stream from the launching platform sensor. Robust performance was demonstrated via the use of a computer simulation. Beam rider guidance is a standard technique that can be employed in weapon postlaunch control.				
14. SUBJECT TERMS Antisubmarine Warfare Combat Control Systems			15. NUMBER OF PAGES 34	
			16. PRICE CODE	
17. SECURITY CLASSIFICATION OF REPORT UNCLASSIFIED	18. SECURITY CLASSIFICATION OF THIS PAGE UNCLASSIFIED	19. SECURITY CLASSIFICATION OF ABSTRACT UNCLASSIFIED	20. LIMITATION OF ABSTRACT SAR	

TABLE OF CONTENTS

	Page
LIST OF TABLES.....	ii
INTRODUCTION.....	1
FORMULATION.....	3
System Description.....	3
Fuzzy Control Subsystem.....	5
Fuzzification Unit.....	5
Rule-Based Unit.....	8
Defuzzification Unit.....	11
Constraint Unit.....	11
System Operation.....	12
SIMULATION RESULTS.....	12
Stationary Bearing Input.....	14
Linear Contact Motion.....	16
Nonlinear Contact Motion.....	20
CONCLUSIONS.....	29
REFERENCES.....	30

LIST OF ILLUSTRATIONS

Figure	Page
1 Beam Rider Trajectory Geometry.....	1
2 Block Diagram of Overall System.....	2
3 Geometry for Guidance Point Control.....	3
4 Overall System Structure for Beam Rider Control.....	4
5 Units that Comprise the Postlaunch Beam Rider Fuzzy Control System.....	4
6 Graphical Representations of the Membership Functions of the Fuzzy Input/Output Sets.....	6
7 Rule-Based Unit.....	8
8 Rule-Based Matrices that Comprise the Rule-Based Unit.....	9
9 Pictorial Example of the Determination of the Composite Implication Function for $B_v - B_c < 0$	10
10 Graphical Representation of the Nonlinear Course Command Constraint.....	11
11 Example of a Fuzzy Beam Rider Trajectory.....	13

LIST OF ILLUSTRATIONS

Figure	Page
12a Guidance Point Bearing Error for Run 1.....	14
12b Change in Error Between Vehicle and Contact Bearings for Run 1.....	15
12c Fuzzy Beam Rider Trajectory for Run 1.....	16
13a Guidance Point Bearing Error for Run 2.....	17
13b Change in Error Between Vehicle and Contact Bearings for Run 2.....	17
13c Fuzzy Beam Rider Trajectory for Run 2.....	18
14a Guidance Point Bearing Error for Run 3.....	19
14b Change in Error Between Vehicle and Contact Bearings for Run 3.....	19
14c Fuzzy Beam Rider Trajectory for Run 3.....	20
15a Guidance Point Bearing Error for Run 4.....	21
15b Change in Error Between Vehicle and Contact Bearings for Run 4.....	21
15c Fuzzy Beam Rider Trajectory for Run 4.....	22
16a Guidance Point Bearing Error for Run 5.....	23
16b Change in Error Between Vehicle and Contact Bearings for Run 5.....	24
16c Fuzzy Beam Rider Trajectory for Run 5.....	24
17a Guidance Point Bearing Error for Run 6.....	25
17b Change in Error Between Vehicle and Contact Bearings for Run 6.....	26
17c Fuzzy Beam Rider Trajectory for Run 6.....	26
18a Guidance Point Bearing Error for Run 7.....	27
18b Change in Error Between Vehicle and Contact Bearings for Run 7.....	28
18c Fuzzy Beam Rider Trajectory for Run 7.....	28

LIST OF TABLES

Table	Page
1 The C and δ Constants.....	7
2 Run Parameters.....	13

A CONSTRAINED FUZZY CONTROLLER FOR BEAM RIDER GUIDANCE

INTRODUCTION

Beam rider guidance is a well understood strategy where the goal is to maintain a vehicle on a trajectory so that its bearing and the bearing of the contact being pursued coincide (figure 1). This technique is a standard technique that can be employed in postlaunch control of a weapon. Although automatic vehicle control schemes that accomplish this objective have been formulated, there has been a reluctance to implement these approaches, retaining man-in-the-loop schemes as the "norm." However, operator loading in complex multi-sensor/multi-vehicle operational scenarios now provides the motivation to develop and employ robust, automatic guidance schemes that allow a system operator to focus attention on tasks of a more supervisory, decision-making nature. This report details the development of a relatively simple fuzzy logic controller and its robust performance.

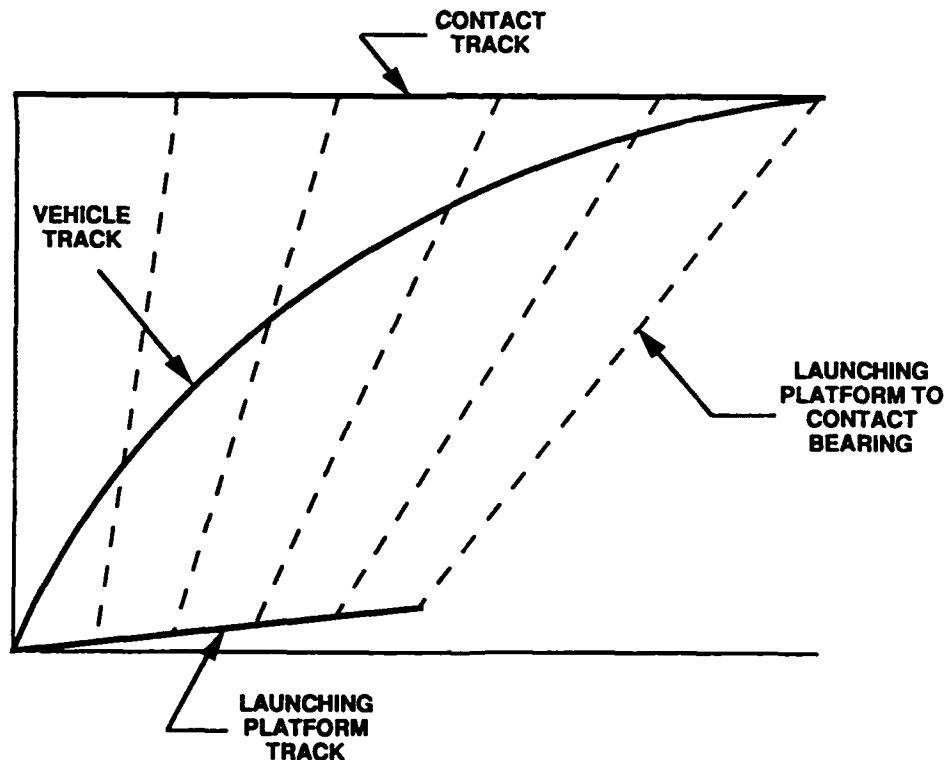


Figure 1. Beam Rider Trajectory Geometry

An overall block diagram of the system being addressed is depicted in figure 2. The problem can be described as one in which a vehicle is launched from a moving platform. Sensors aboard the platform obtain noisy, time-varying measurements of the bearing to the contact. A two-way communication link is available between the vehicle and launcher; this provides the mechanism for providing postlaunch control of the vehicle and for the vehicle to provide the feedback data necessary to determine its position and thereby bearing. The measured bearing to the contact, along with the position data on the vehicle, is used to determine the discrete commands that must be sent to the vehicle. Here, different than the classical beam rider depicted in figure 1, the objective is to provide control so that a point (which is a specified distance in front of the vehicle and along its longitudinal axis) is maintained on the bearing between launcher and contact (see figure 3). An example of this type of control is in the situation where a vehicle is acoustically searching and it is desired to guide a point that corresponds to good acoustic behavior. No restrictions are placed on either launcher or contact motion. Examination of the problem indicates the sensitivity of guidance point control to vehicle course changes. Here it is clear that for the same vehicle course delta, significantly different movement of the guidance point occurs for different guidance distances.

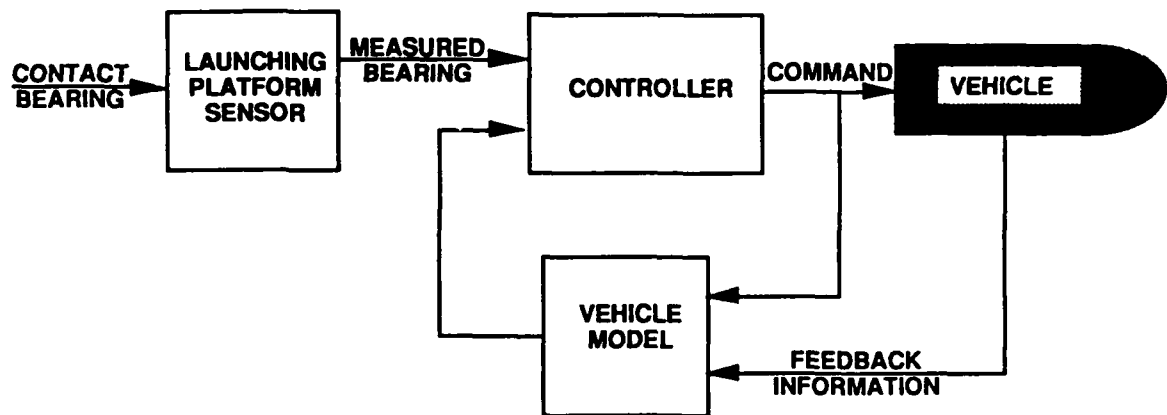


Figure 2. Block Diagram of Overall System

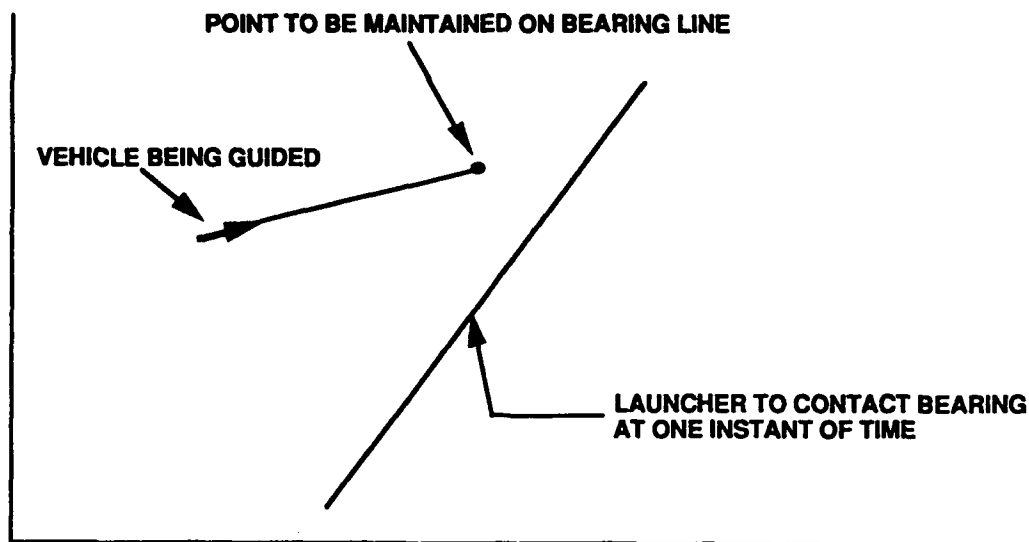


Figure 3. Geometry for Guidance Point Control

FORMULATION

SYSTEM DESCRIPTION

The overall system for beam rider control is shown in figures 4 and 5. The trajectory model subsystem computes both the error (e_{gp}) between the contact bearing (B_c) and the vehicle guidance point bearing (B_{gp}) and the change in error (Δe_v) between the vehicle bearing (B_v) and contact bearing. The contact bearing is a noisy data stream obtained from the launching platform's sensors and the vehicle bearing is provided by the vehicle mathematical model. The fuzzy subsystem uses these variables ($e_{gp}, \Delta e_v$) to determine the control (u) necessary to maintain the vehicle guidance point on the contact bearing. A constraint is applied to u to ensure that a command is never given such that the vehicle would have a velocity component in the direction of the launching platform at any time during postlaunch control. The value of this constraint is continually computed because it is a function of the dynamics of the situation. The resultant command is sent to the weapon via the wire and to the vehicle model and, together with the vehicle feedback data, is used to update the vehicle kinematics.

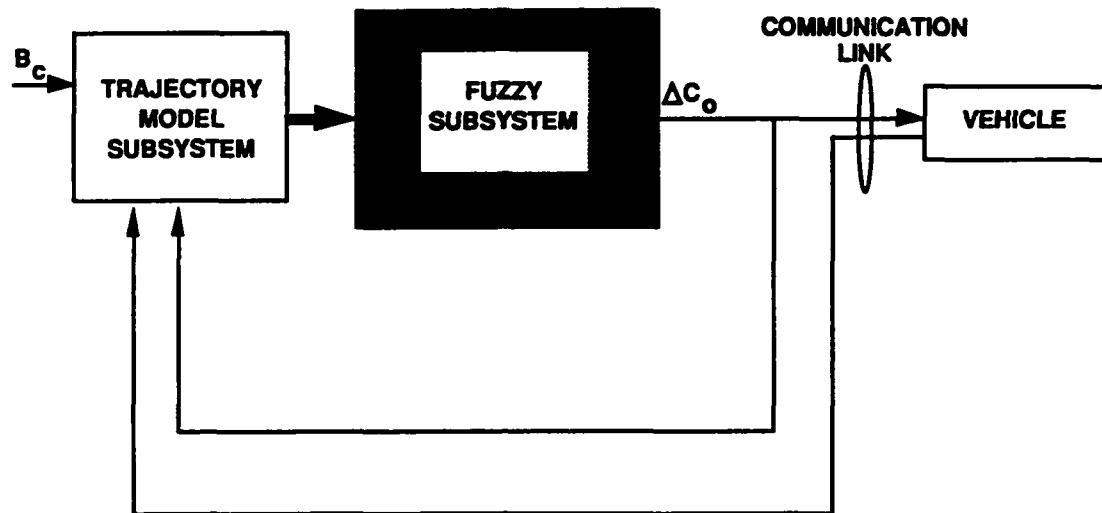


Figure 4. Overall System Structure for Beam Rider Control

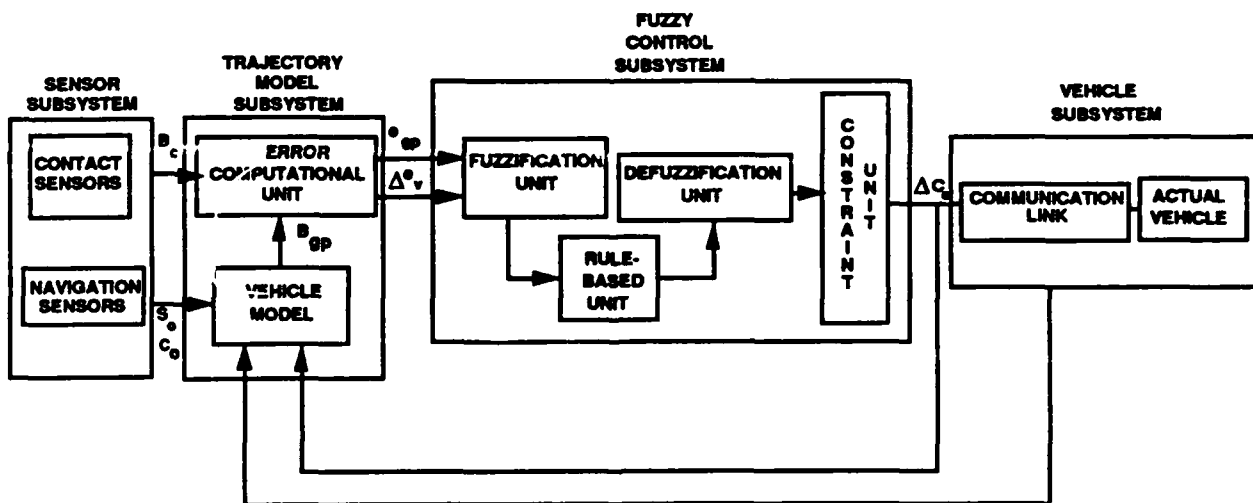


Figure 5. Units that Comprise the Postlaunch Beam Rider Fuzzy Control System

FUZZY CONTROL SUBSYSTEM

The functional elements comprising the fuzzy control system are the fuzzification unit, rule-based unit, defuzzification unit, and the constraint unit. A description of each of these units follows.

Fuzzification Unit

The fuzzification unit takes crisp inputs and encodes them into fuzzy sets. The input variables associated with the system are x_1 (the guidance point bearing error) and x_2 (the change in angle between the vehicle bearing and the contact bearing) and are defined as

$$x_1 = e_{gp} = B_{gp} - B_c ,$$

$$x_2 = \Delta e_v = |B_v - B_c|_k - |B_v - B_c|_{k-1} .$$

Note, the following fuzzy control was derived for $-90 \leq B_v \leq 90$ and $-90 \leq B_c \leq 90$.

Encoding of the system inputs requires mapping crisp numerical measurements into fuzzy set representations or linguistic variables. The universes of discourse for input x_1 and x_2 are composed of the seven and five linguistic variables, respectively, defined by the following term sets:

$$T(x_1) = \{T^1_{x_1}, T^2_{x_1}, T^3_{x_1}, T^4_{x_1}, T^5_{x_1}, T^6_{x_1}, T^7_{x_1}\} = (NL, NM, NS, ZE, PS, PM, PL) ,$$

$$T(x_2) = \{T^1_{x_2}, T^2_{x_2}, T^3_{x_2}, T^4_{x_2}, T^5_{x_2}\} = (NL, NS, ZE, PS, PL) ,$$

where

NL - Negative Large, NM - Negative Medium, NS - Negative Small,
ZE - Zero, PS - Positive Small, PM - Positive Medium, and
PL - Positive Large.

The set of membership functions $\mu(x_1)$ corresponding to input x_1 and the set of membership functions $\mu(x_2)$ corresponding to input x_2 ,

$$\mu(x_1) = \{\mu^1_{x_1}, \mu^2_{x_1}, \mu^3_{x_1}, \mu^4_{x_1}, \mu^5_{x_1}, \mu^6_{x_1}, \mu^7_{x_1}\} ,$$

$$\mu(x_2) = \{\mu^1_{x_2}, \mu^2_{x_2}, \mu^3_{x_2}, \mu^4_{x_2}, \mu^5_{x_2}\} ,$$

are depicted in figures 6a and 6b, respectively, and are given by the following equations:

1. For $j = 1$ and $i = 2, 3, 4, 5, 6$, and for $j = 2$ and $i = 2, 3, 4$:

$$\mu^i_{x_j} = -(|x_j - C^i_{x_j}|) / \delta^i_{x_j} + 1 \quad \text{for } C^i_{x_j} - \delta^i_{x_j} \leq x_j \leq C^i_{x_j} + \delta^i_{x_j} ,$$

$$\mu^i_{x_j} = 0 \quad \text{for } C^i_{x_j} - \delta^i_{x_j} > x_j > C^i_{x_j} + \delta^i_{x_j} .$$

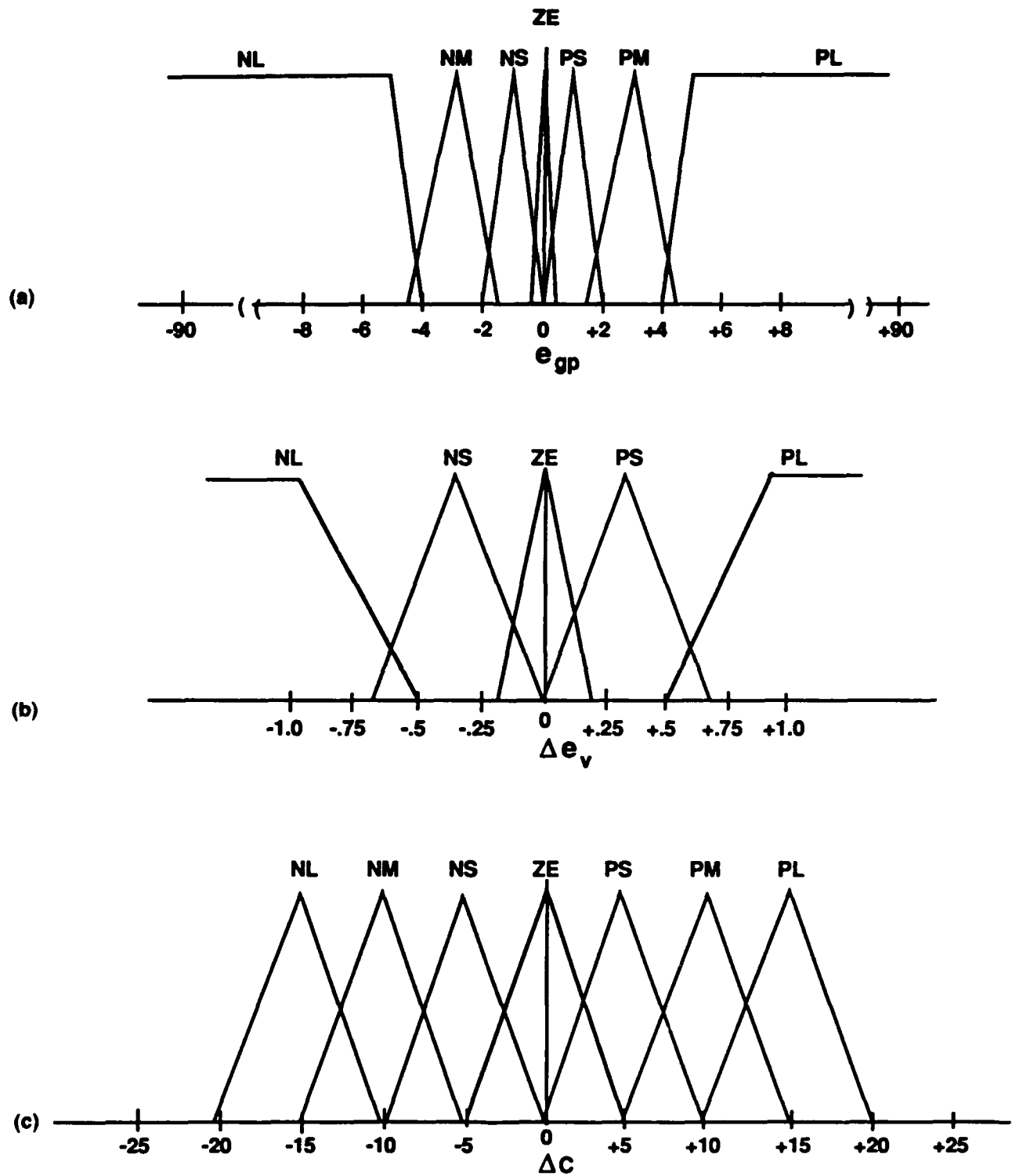


Figure 6. Graphical Representations of the Membership Functions of the Fuzzy Input/Output Sets

2. For $j = 1$ and $i = 1, 7$ and for $j = 2$ and $i = 1, 5$:

$$\begin{aligned} \mu_{xj}^i &= -(|x_j - C_{xj}^i|) / \delta_{xj}^i + 1 && \text{for } a^i C_{xj}^i \geq a^i x_j \geq a^i (C_{xj}^i - a^i \delta_{xj}^i) , \\ \mu_{xj}^i &= 1 && \text{for } a^i C_{xj}^i < a^i x_j , \\ \mu_{xj}^i &= 0 && \text{for } a^i (C_{xj}^i - a^i \delta_{xj}^i) > a^i x_j , \end{aligned}$$

where $a^i = 1$, except for $i = 1$, where $a^1 = -1$.

The system output variable or control variable is the vehicle course command (ΔC); the universe of discourse for ΔC is composed of the seven linguistic variables defined by the following term set:

$$T(\Delta C) = \{T_{\Delta C}^1, T_{\Delta C}^2, T_{\Delta C}^3, T_{\Delta C}^4, T_{\Delta C}^5, T_{\Delta C}^6, T_{\Delta C}^7\} = (NL, NM, NS, ZE, PS, PM, PL) .$$

The set of membership functions $\mu(\Delta C)$ corresponding to output ΔC ,

$$\mu(\Delta C) = \{\mu_{\Delta C}^1, \mu_{\Delta C}^2, \mu_{\Delta C}^3, \mu_{\Delta C}^4, \mu_{\Delta C}^5, \mu_{\Delta C}^6, \mu_{\Delta C}^7\} ,$$

is depicted in figure 6c and given by the following equation:

For $i = 1, 2, 3, 4, 5, 6, 7$:

$$\begin{aligned} \mu_{\Delta C}^i &= -(|\Delta C - C_{\Delta C}^i|) / \delta_{\Delta C}^i + 1 && \text{for } C_{\Delta C}^i - \delta_{\Delta C}^i \leq \Delta C \leq C_{\Delta C}^i + \delta_{\Delta C}^i , \\ \mu_{\Delta C}^i &= 0 && \text{for } C_{\Delta C}^i - \delta_{\Delta C}^i > \Delta C > C_{\Delta C}^i + \delta_{\Delta C}^i . \end{aligned}$$

The values of the membership equation constants C and δ are given in table 1.

Table 1. The C and δ Constants

i	$\mu(x1)$		$\mu(x2)$		$\mu(\Delta C)$	
	C_{x1}^i	δ_{x1}^i	C_{x2}^i	δ_{x2}^i	$C_{\Delta C}^i$	$\delta_{\Delta C}^i$
1	-5.0	1.0	-0.95	0.45	-15.0	5.0
2	-3.0	1.5	-0.3375	0.3375	-10.0	5.0
3	-1.0	1.0	0.0	0.1875	-5.0	5.0
4	0.0	0.4	0.3375	0.3375	0.0	5.0
5	1.0	1.0	0.95	0.45	5.0	5.0
6	3.0	1.5	--	--	10.0	5.0
7	5.0	1.0	--	--	15.0	5.0

Rule-Based Unit

Figure 7 is a depiction of the fuzzy rule-based unit that consists of the heuristic relationships (i.e., IF THEN rules) between the fuzzy inputs and outputs and fuzzy implication operations.

The matrices in figure 8 define the heuristic relationships that resulted from the translation of an understanding of bearing rider torpedo guidance to a set of rules. Each entry in these matrices corresponds to a "rule" and defines the input/output relationship between the fuzzy variables, e.g., the rule defined by the entry in the first row and first column of the first matrix is

IF e_{gp} is NL AND Δe_v is NL AND $(B_v - B_c)$ is positive THEN ΔC is PL .

The generation of these matrices did not require a mathematical description of system dynamics but rather intuitive knowledge of system behavior. Experimentation was used to refine the original rule set to that of figure 8. The two matrices define a total of 70 rules, 35 rules for each sign condition of $(B_v - B_c)$.

For each fuzzy rule that is fired, there is a fuzzy implication and an associated fuzzy implication function. The determination of the fuzzy implication functions is explained through the use of an example. The following two rules in the second matrix are fired:

- (1) IF x_1 is $T^4_{x_1}$ AND x_2 is $T^3_{x_2}$ THEN ΔC is $T^4_{\Delta C}$.
- (2) IF x_1 is $T^5_{x_1}$ AND x_2 is $T^4_{x_2}$ THEN ΔC is $T^3_{\Delta C}$.

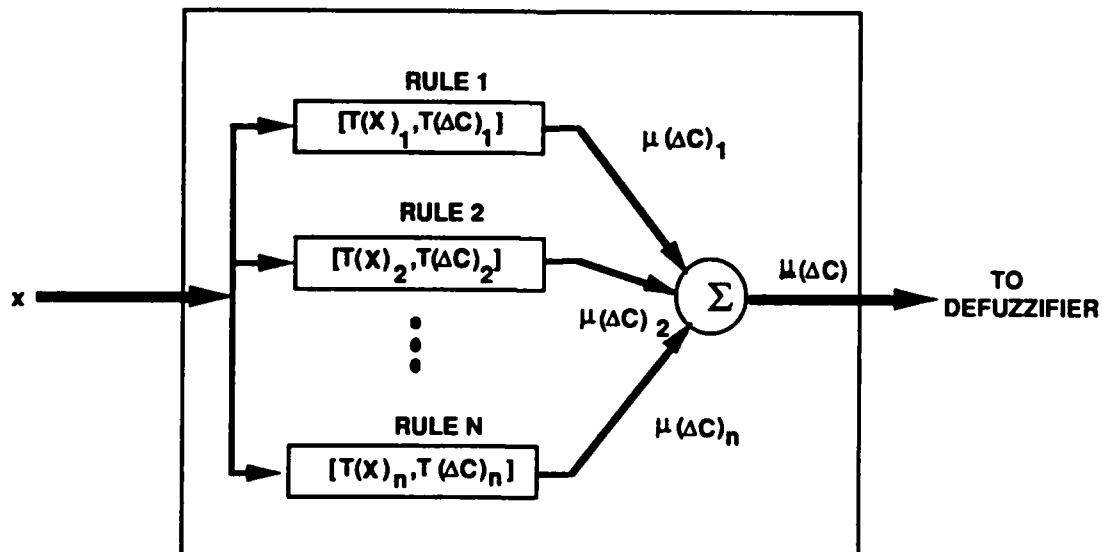


Figure 7. Rule-Based Unit

		e_{gp}						
		NL	NM	NS	ZE	PS	PM	PL
Δe_v	NL	PL	PL	PL	PS	ZE	NM	NL
	NS	PL	PM	PS	ZE	NS	NM	NL
	ZE	PL	PM	PS	ZE	NS	NM	NL
	PS	PL	PM	PS	NS	NM	NL	NL
	PL	PL	PS	ZE	NS	NL	NL	NL

		e_{gp}						
		NL	NM	NS	ZE	PS	PM	PL
Δe_v	NL	PL	PM	ZE	NS	NL	NL	NL
	NS	PL	PM	PS	ZE	NS	NM	NL
	ZE	PL	PM	PS	ZE	NS	NM	NL
	PS	PL	PL	PM	PS	NS	NM	NL
	PL	PL	PL	PL	PS	ZE	NS	NL

*Figure 8. Rule-Based Matrices that Comprise the Rule-Based Unit
(Top: $B_v - B_c > 0$; Bottom: $B_v - B_c < 0$)*

The numerical strength of the output of rules 1 and 2 can be expressed respectively as

$$\zeta(1) = y_{x1}^4 \wedge y_{x2}^3 = \min(y_{x1}^4, y_{x2}^3),$$

$$\zeta(2) = y_{x1}^5 \wedge y_{x2}^4 = \min(y_{x1}^5, y_{x2}^4),$$

where y_{xj}^i is μ_{xj}^i evaluated at a specific value of $x_j(t)$ at time t , and \wedge denotes fuzzy minimum.

The inferred output control function from the first rule is $\zeta(1)\mu^4_{\Delta C}$; similarly, the inferred function from the second rule is $\zeta(2)\mu^3_{\Delta C}$.

$\zeta(1)\mu^4_{\Delta C} = \mu(\Delta C)(1)$ = the output control function for rule 1 defined by $\mu^4_{\Delta C}$ multiplied by the value $\zeta(1)$,

$\zeta(2)\mu^3_{\Delta C} = \mu(\Delta C)(2)$ = the output control function for rule 2 defined by $\mu^3_{\Delta C}$ multiplied by the value $\zeta(2)$.

The output composite implication function ($\mu(\Delta C)$) of the rule-based unit for this example is expressed as

$$\mu(\Delta C) = \mu(\Delta C)(1) + \mu(\Delta C)(2).$$

The determination of the composite implication function is shown graphically in figure 9 for the above example.

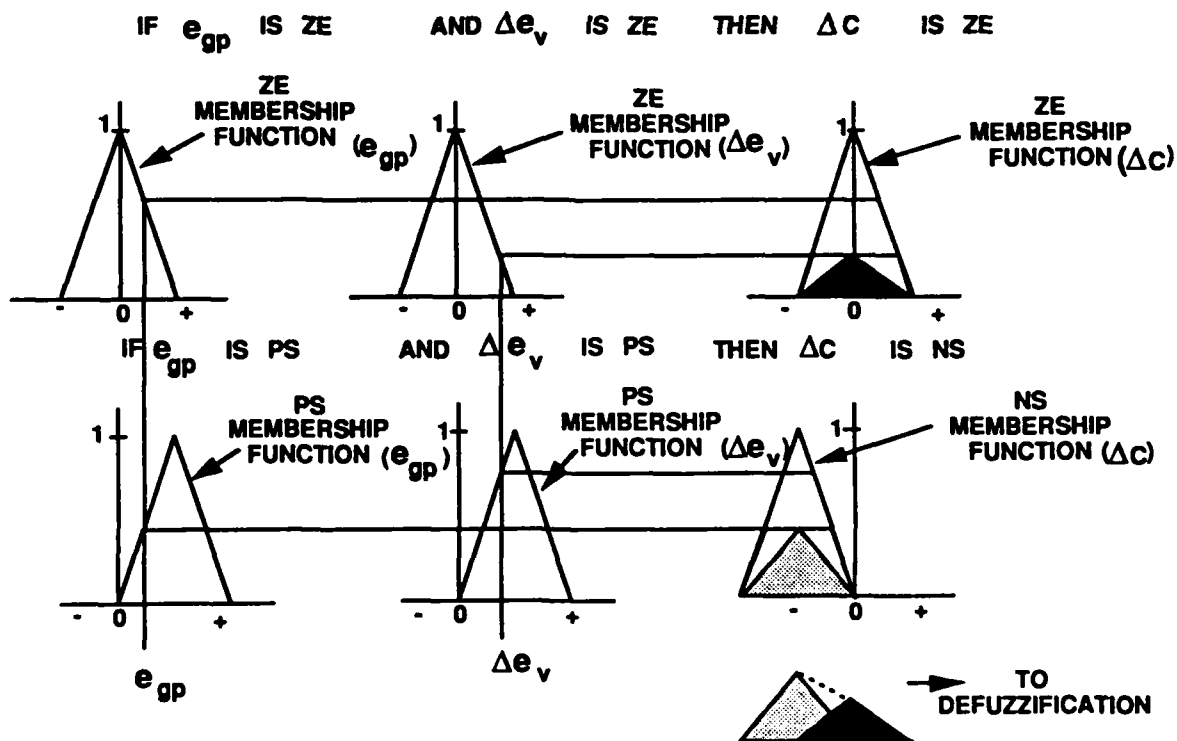


Figure 9. Pictorial Example of the Determination of the Composite Implication Function for $B_v - B_c < 0$

Defuzzification Unit

The defuzzification unit takes the fuzzy outputs from the rule-based unit and decodes them into a crisp output that is acceptable for use in vehicle control. This unit employs a strategy that maps fuzzy control actions defined over an output universe of discourse (see figure 6c) into a space of crisp control actions (i.e., course commands). The method of defuzzification used in this application is the centroid method. The centroid of the composite function is used as the crisp control value and is computed as follows:

$$\Delta C = \Sigma_k \{ (\zeta(k) C_{\Delta C(k)}) I_{\Delta C(k)} \} / \Sigma_k \zeta(k) I_{\Delta C(k)} ,$$

where Σ_k indicates summation over all the rules fired.

$I_{\Delta C(k)}$ and $C_{\Delta C(k)}$ are defined as the respective area and centroid of the k th rule consequent set membership function.

Constraint Unit

The constraint unit interrogates the control commands coming from the defuzzification unit to determine if these commands exceed limits that are governed by the tactical situation. Figure 10 is a graphical representation of this unit and the value of the vehicle course command limits L_1 and L_2 are defined as follows:

$$L_1 = B_v + 90^\circ - (C_{vm})_{k-1} ,$$

$$L_2 = B_v - 90^\circ - (C_{vm})_{k-1} ,$$

where $(C_{vm})_{k-1}$ is the vehicle course from the last update cycle.

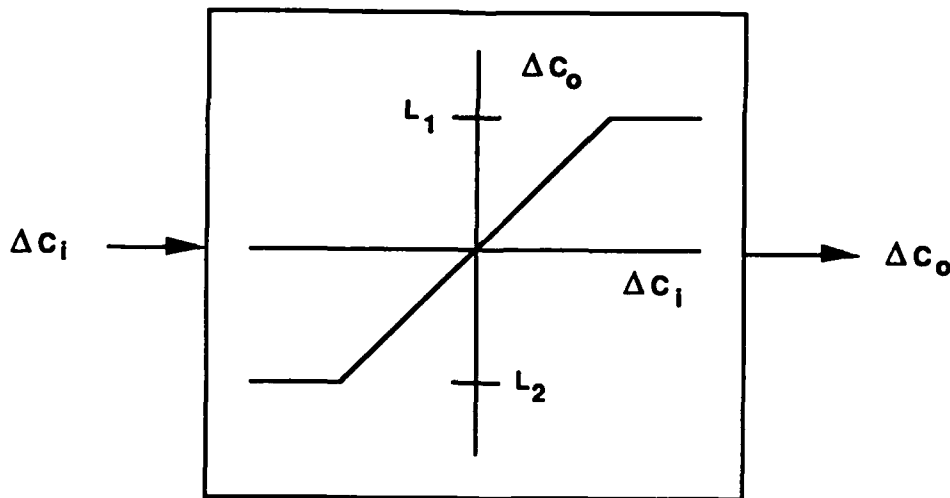


Figure 10. Graphical Representation of the Nonlinear Course Command Constraint

These limits assume no initial vehicle velocity component in the direction of the firing vessel and ensure that the trajectory of the vehicle that would result from the addition of the fuzzy control system commands is such that there is no vehicle velocity component in the direction of the firing vessel at any time during postlaunch guidance operation. When the computed command exceeds the limit, only the portion of the command that will result in the vehicle being on a trajectory that is perpendicular to the vehicle bearing line is sent to the weapon. Because the course command limits in the constraint unit are dependent on the tactical situation, these limits are determined every update cycle.

SYSTEM OPERATION

In the operation of the new fuzzy control beam rider system, the contact bearing is combined with the vehicle guidance point bearing to form the guidance bearing error (e_{gp}). The absolute value of the angle between the vehicle bearing and the contact bearing from the previous update cycle is subtracted from the current angle's absolute value to form the change in angle between the vehicle bearing and the contact bearing (Δe_v). The vehicle guidance point bearing error and the change in angle between the vehicle bearing and the contact bearing are converted to fuzzy inputs by the fuzzification unit. Based on these inputs and the sign of the angle between the vehicle bearing and the contact bearing, the fuzzy rule-based unit invokes all the appropriate rules to determine the resultant fuzzy output actions. These actions are combined and sent to the defuzzification unit. The composite fuzzy output is converted to a numerical course command. The constraint unit interrogates this command to determine if the command, or any portion of it, can be issued to the weapon. The constraint unit course command output is automatically sent to the actual vehicle over the wire communication link and also provided to update the vehicle model in the SCCS. The process described herein is not a one-time postlaunch activity, but it goes on continually throughout the postlaunch encounter.

SIMULATION RESULTS

A computer simulation was developed that includes the contact vehicle model, launching ship model, and a model of the vehicle being guided. The fuzzy system for vehicle control was implemented and test runs were made to demonstrate and analyze performance. The transient and steady-state responses were obtained for the cases of a stationary contact and both linear and nonlinear contact motion. An example of a fuzzy beam rider trajectory is shown in figure 11; the problem parameters are indicated on this figure. A large number of simulation runs were made to examine performance. Table 2 contains the values for the selected runs included in the report. In all cases, the initial range to the contact was 5000 yards and the initial bearing to the contact was 90° .

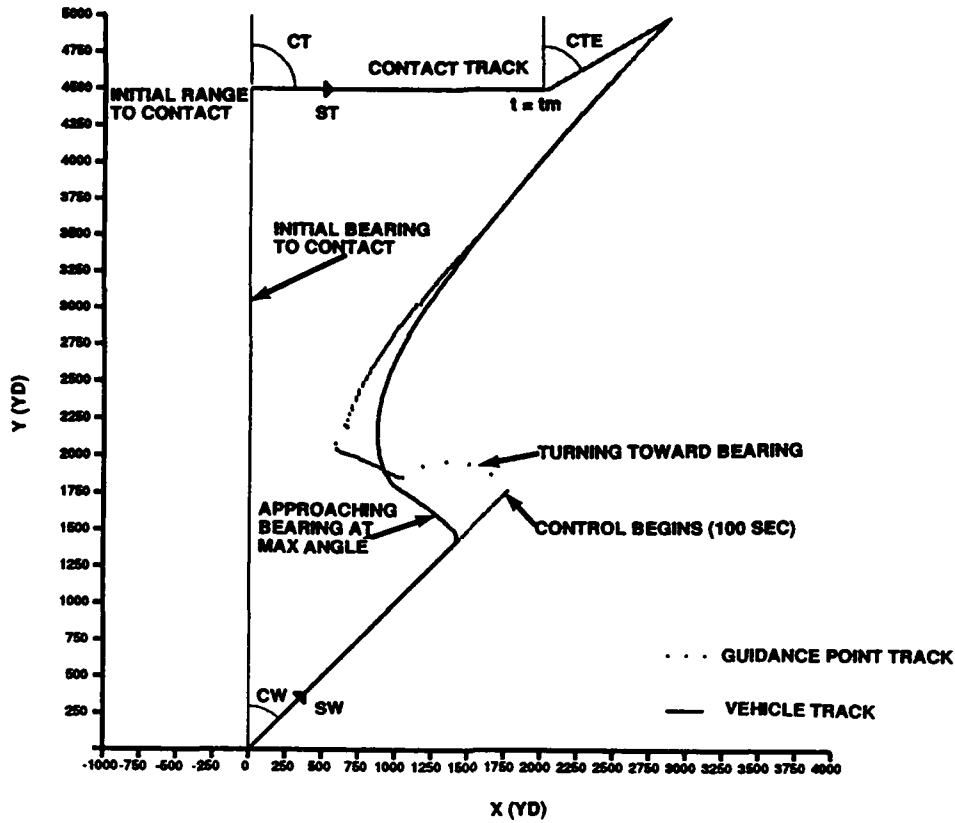


Figure 11. Example of a Fuzzy Beam Rider Trajectory

Table 2. Run Parameters

Run No.	Vehicle			Contact				
	SW (yd/sec)	CWI (deg)	GD (yd)	ST (yd/sec)	CT (deg)	STE (yd/sec)	CTE (deg)	t_m (sec)
1	20	45	500	0	90	--	--	--
2	20	45	500	10	90	--	--	--
3	20	45	500	10	-90	--	--	--
4	20	45	500	10	90	15	-30	210
5	20	45	500	10	90	15	120	210
6	20	45	500	10	90	15	-30	125
7	20	45	500	10	90	15	120	125

Three general types of geometries were selected to illustrate the behavior of the fuzzy control system: a stationary bearing input (run 1), linear contact motion (runs 2 and 3), and nonlinear (evasive) contact motion (runs 4, 5, 6, and 7).

STATIONARY BEARING INPUT

The first situation that is examined is that of a stationary contact and launching platform. In this case, a vehicle is launched on a course of 45° and proceeds on this course for 100 seconds; at this time, control of the vehicle begins. Because of the stationarity of the platforms, this geometry produces a step-type input (constant bearing) to the control system. Figure 12 (a,b,c) shows the output plots for run 1; figure 12a depicts the bearing error, i.e., the difference between the contact bearing and the vehicle guidance point bearing. Note the change in slope of the bearing error at approximately 106 seconds; this is indicative of the vehicle reaching its constrained course; i.e., a course perpendicular to the vehicle's bearing such that the vehicle does not have a component of velocity in the direction of the launch platform. Prior to this point, the vehicle is being commanded to turn toward the contact bearing from its initial launch course of 45° . After this point, the commanded course is such that the vehicle is closing on the contact bearing at the maximum allowable closure rate. The result is that the vehicle approaches the contact bearing on a constant radius trajectory from the launch platform while turning at a constant rate. At 159 seconds, the vehicle guidance point crosses the contact bearing line and vehicle course commands are issued in the appropriate direction to minimize overshoot. The controller is able to always maintain the vehicle guidance point within 0.5° of the bearing line; after 170 seconds, the error is less than 0.25° .

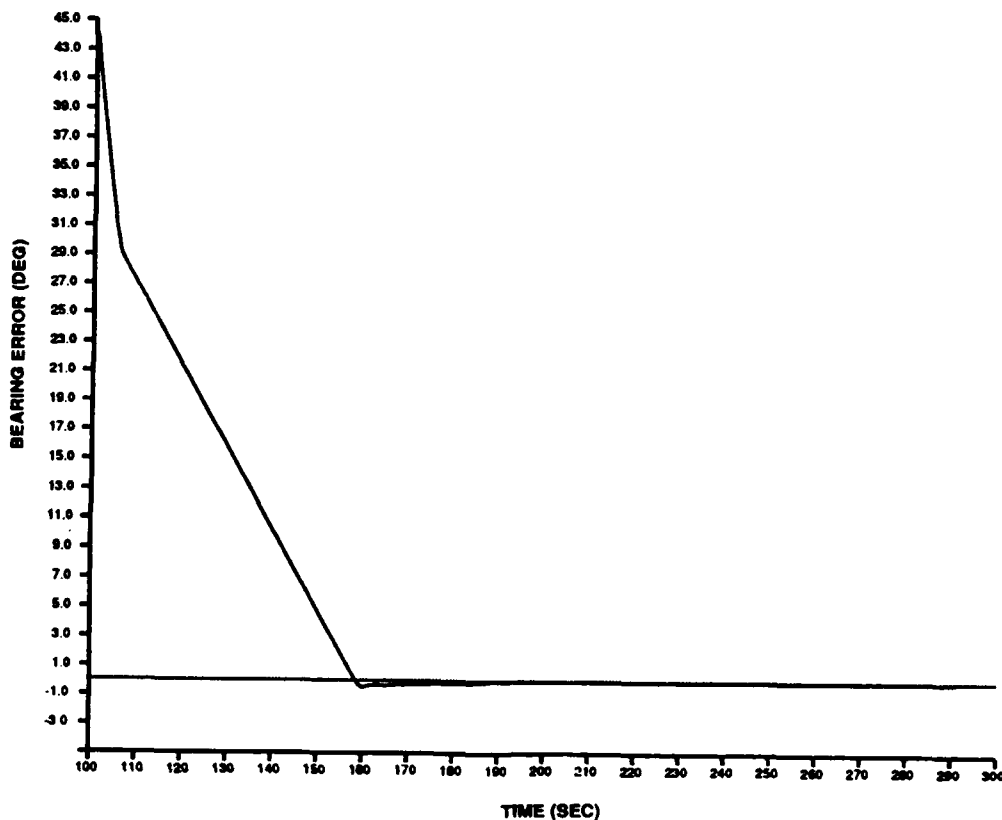


Figure 12a. Guidance Point Bearing Error for Run 1

Figure 12b is a plot of x_2 as a function of time. This shows the behavior of the difference of the absolute value of weapon bearing minus contact bearing over a time interval of 1 second. The error (x_2) remains constant (indicating a linear reduction in the x_1 error) as the vehicle approaches the contact bearing at the maximum allowable angle. After the vehicle guidance point crosses the stationary contact bearing line, the magnitude of x_2 decreases, demonstrating the required behavior to allow the vehicle guidance point to fair in and remain close to the contact bearing line. Because, for this run, the contact and launching platform are stationary, the bearing line is fixed in time and therefore x_2 asymptotically approaches zero as the vehicle course approaches coincidence with the bearing to the contact. Figure 12c shows the trajectories of the contact, vehicle, and vehicle guidance point (launching platform stationary at 0,0 coordinates). These results reflect excellent behavior for the vehicle bearing rider application.

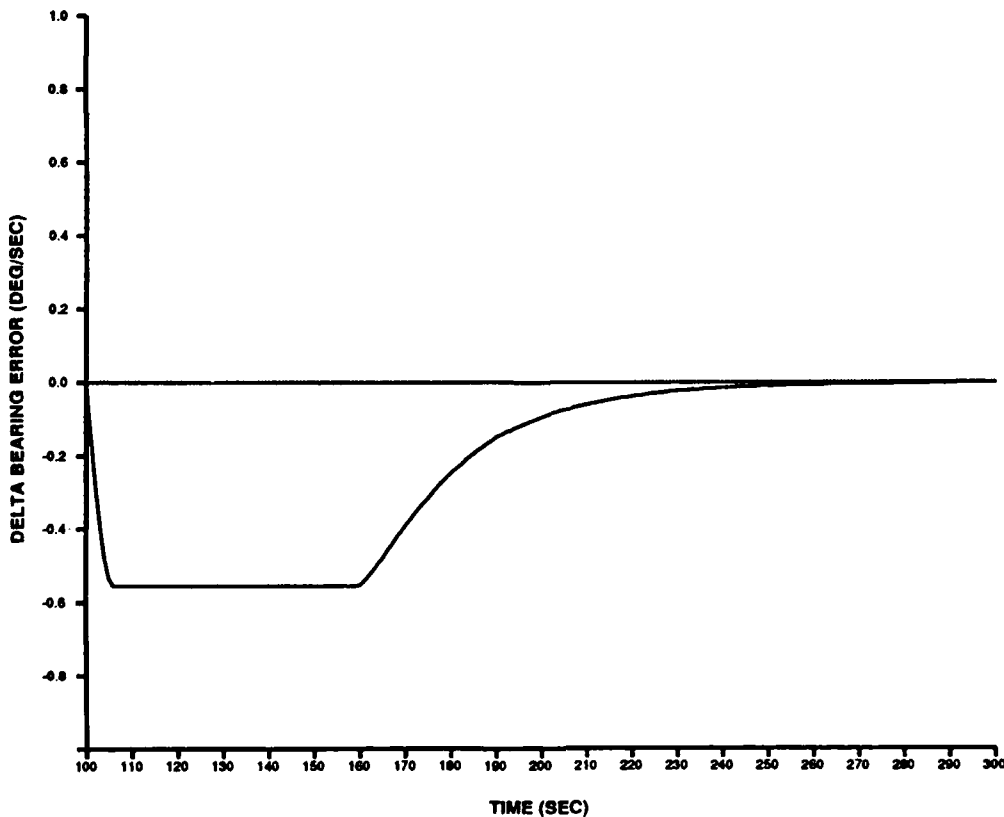


Figure 12b. Change in Error Between Vehicle and Contact Bearings for Run 1

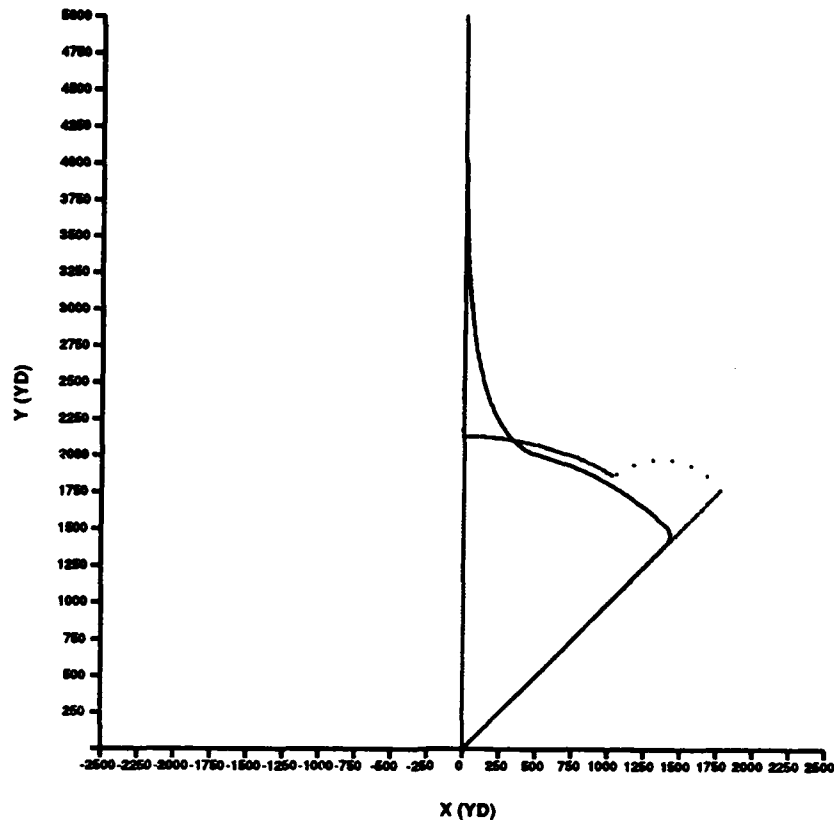


Figure 12c. Fuzzy Beam Rider Trajectory for Run 1

LINEAR CONTACT MOTION

The situation examined in runs 2 and 3 is that of linear contact motion, i.e., a contact that moves on a constant course at a constant speed. This type of contact motion results in a nonlinear, arctangent form, bearing input to the control system.

In run 2 (figures 13a, 13b, and 13c), the vehicle is launched at 45° and the course of the target is such that the contact bearing is moving toward the vehicle. Figure 13a, the x_1 error, demonstrates that the nonlinear time varying bearing input poses no problem to the control system. At 132 seconds, the vehicle guidance point crosses the contact bearing line and at 51 seconds after initiation of control (about 151 seconds in figure 13a), the guidance point is steadily maintained with 0.25° of the changing contact bearing. The times to reach the initial contact bearing crossing and steady state are shorter than in run 1; this is due to the increasing closure rate caused by the contact's motion. Figure 13b exhibits behavior similar to that previously discussed with the exception that the error changes direction at 174 seconds. This behavior is a result of the fact that the vehicle must cross the contact bearing line to achieve the relationship required for true steady-state beam rider operation, i.e., the vehicle must be in a position where it is chasing the bearing line. The trajectory plot for run 2 is given in figure 13c.

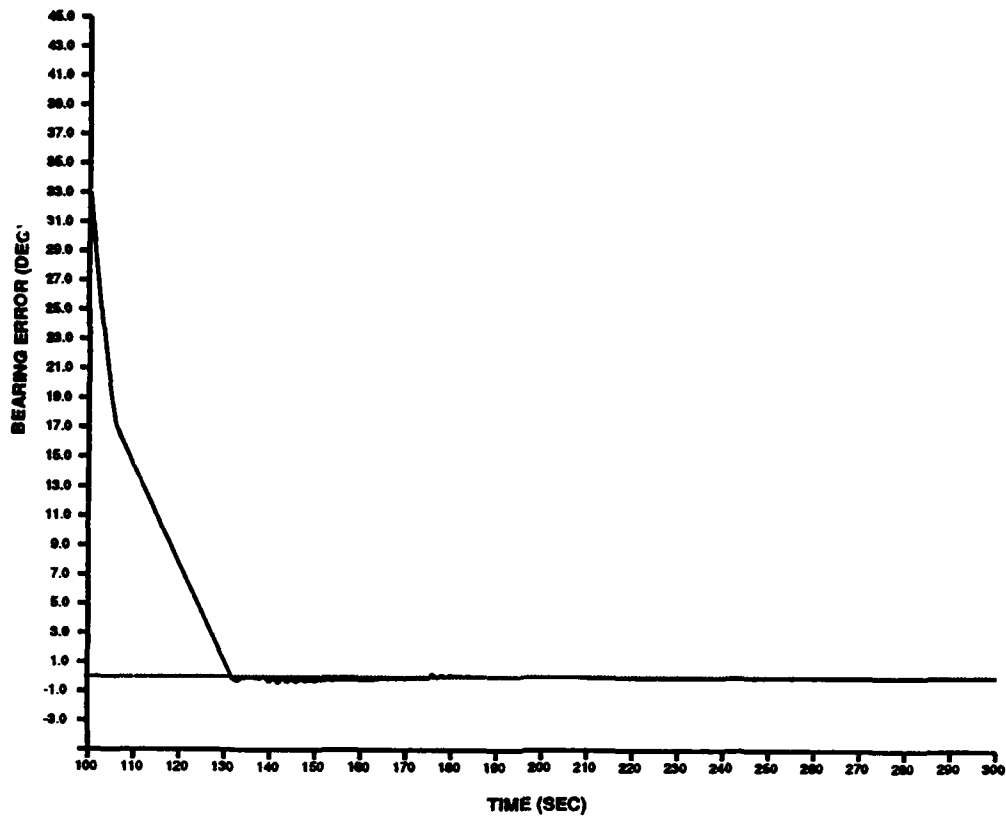


Figure 13a. Guidance Point Bearing Error for Run 2

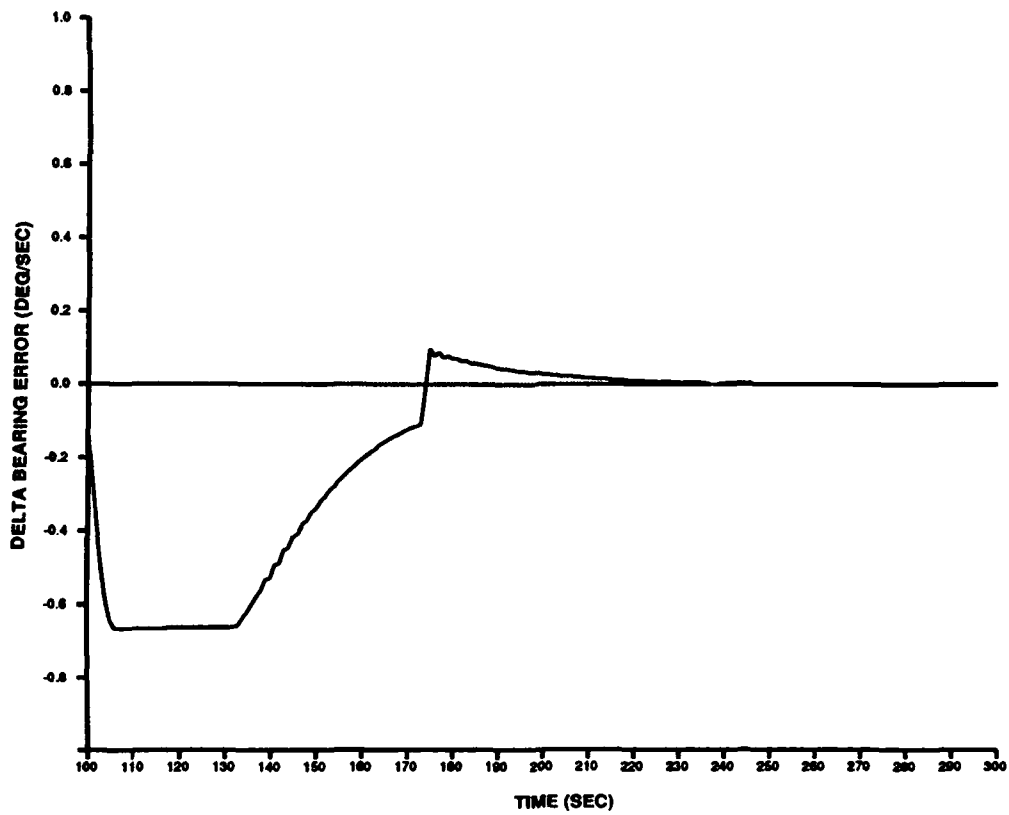


Figure 13b. Change in Error Between Vehicle and Contact Bearings for Run 2

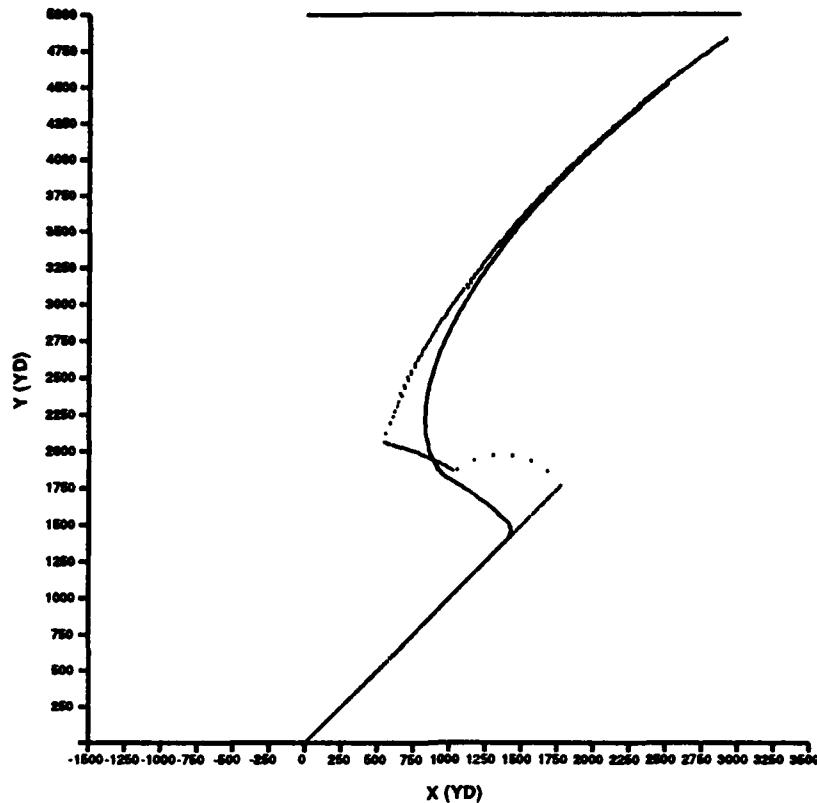


Figure 13c. Fuzzy Beam Rider Trajectory for Run 2

In run 3, the vehicle is launched on the same initial course; however, the target is moving on a course such that the bearing is moving away from the vehicle. From figure 14a, it is apparent that it takes longer for the vehicle guidance point to cross the contact bearing line (crosses at 198 seconds) and about twice as long for the error to decrease to 0.25° (106 versus 51 seconds after initiation of control). This however, is not caused by any deficiency in the controller, but rather to the fact that the contact is moving in the same direction as the vehicle (i.e., the vehicle's closure rate on the contact bearing is reduced). Figure 14b is similar in behavior to that of 12b because the vehicle does not have to cross the bearing line to attain its steady-state orientation.

The trajectory plot for run 3 is given in figure 14c; as in the stationary bearing case, good controller behavior is exhibited for vehicle bearing rider operation in the contact linear motion runs. In figure 14c, the constant radius trajectory is clearly evident during the period when the vehicle is closing on the contact bearing at the maximum allowable closure rate (vehicle course constraint imposed).

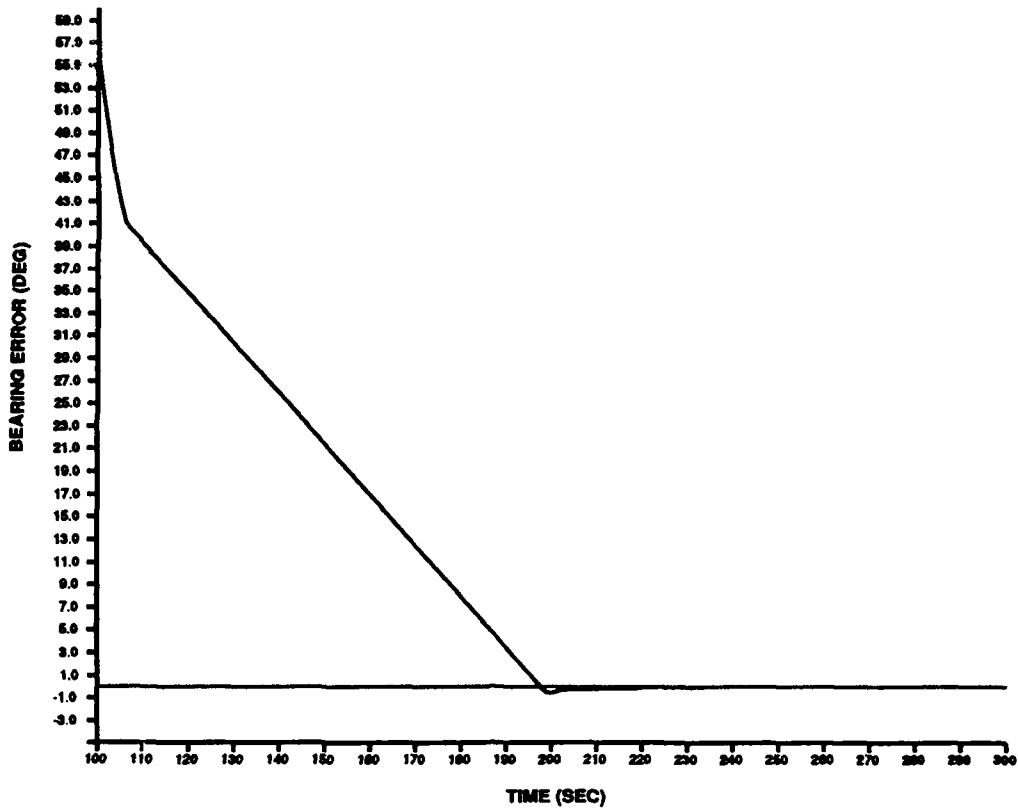


Figure 14a. Guidance Point Bearing Error for Run 3

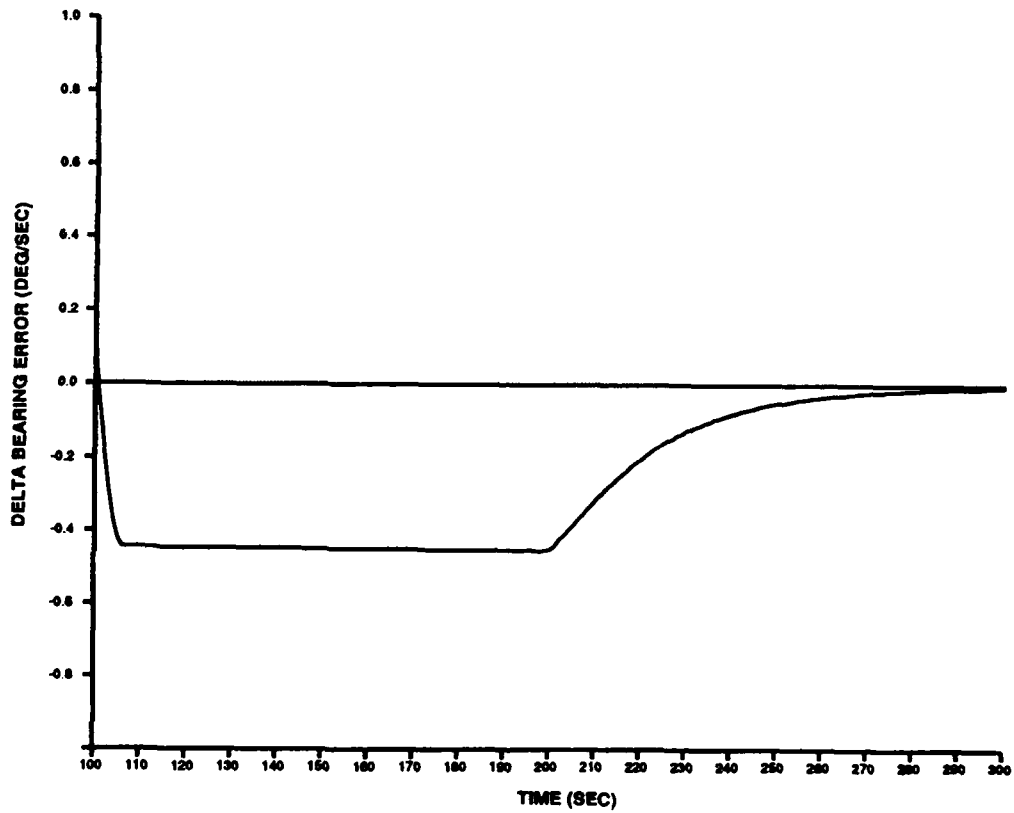


Figure 14b. Change in Error Between Vehicle and Contact Bearings for Run 3

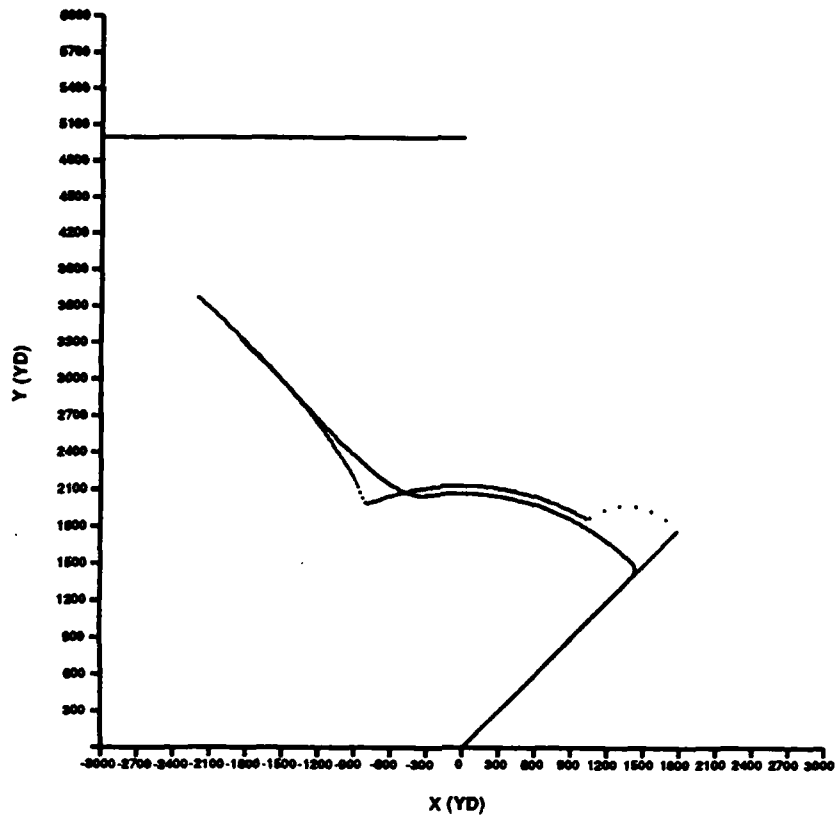


Figure 14c. Fuzzy Beam Rider Trajectory for Run 3

NONLINEAR CONTACT MOTION

The final type of contact motion examined is that of a contact that moves on a constant course at a constant speed for a given period of time and then maneuvers/evades to a different course and speed.

In run 4, the contact maneuvers from a 90° course to a -30° course; this action is representative of a contact attempting to escape a vehicle. The vehicle is launched at a 45° angle leading the bearing line. Control begins at 100 seconds and the behavior is similar to run 2 up to the maneuver. The contact then maneuvers at 210 seconds, changing both its course and speed. Referring to figure 15a, it is apparent that the radical contact velocity change has negligible effect on the ability of the controller to maintain the guidance point on the bearing line. In figure 15b, the contact maneuver is apparent. The evasive maneuver results in a reversal of direction for the motion of the contact bearing line; i.e., before the maneuver, the contact bearing line is increasing (positive contact bearing rate) while after the maneuver, the contact bearing is decreasing (negative contact bearing rate).

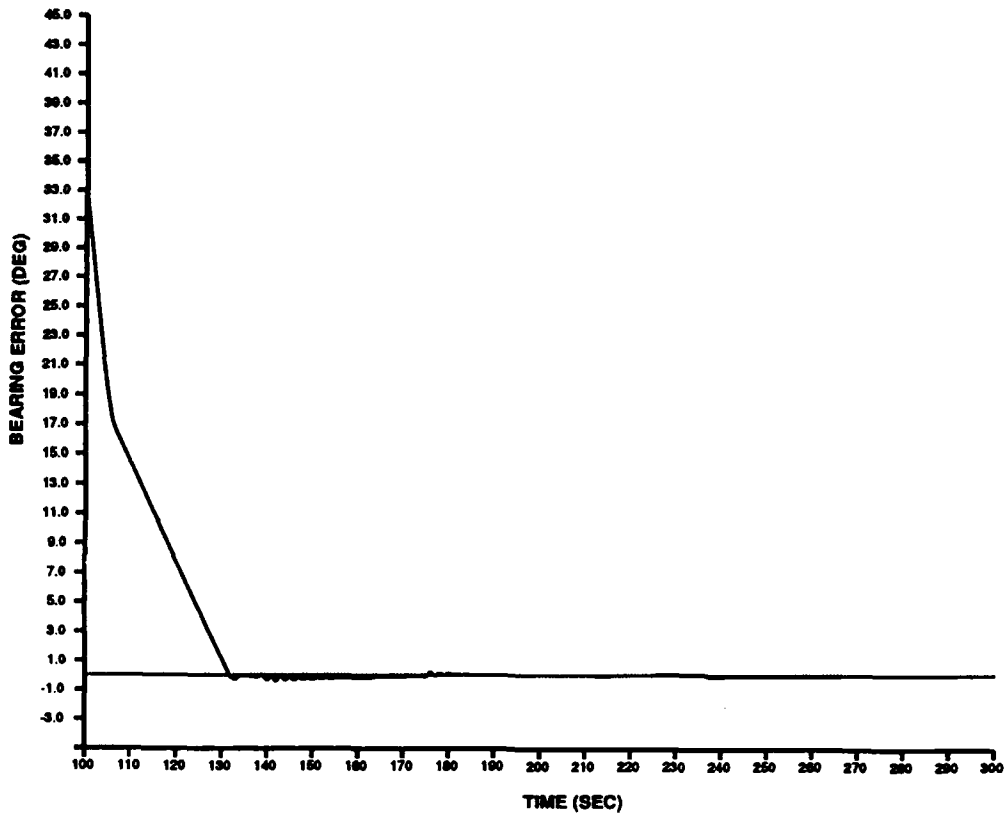


Figure 15a. Guidance Point Bearing Error for Run 4

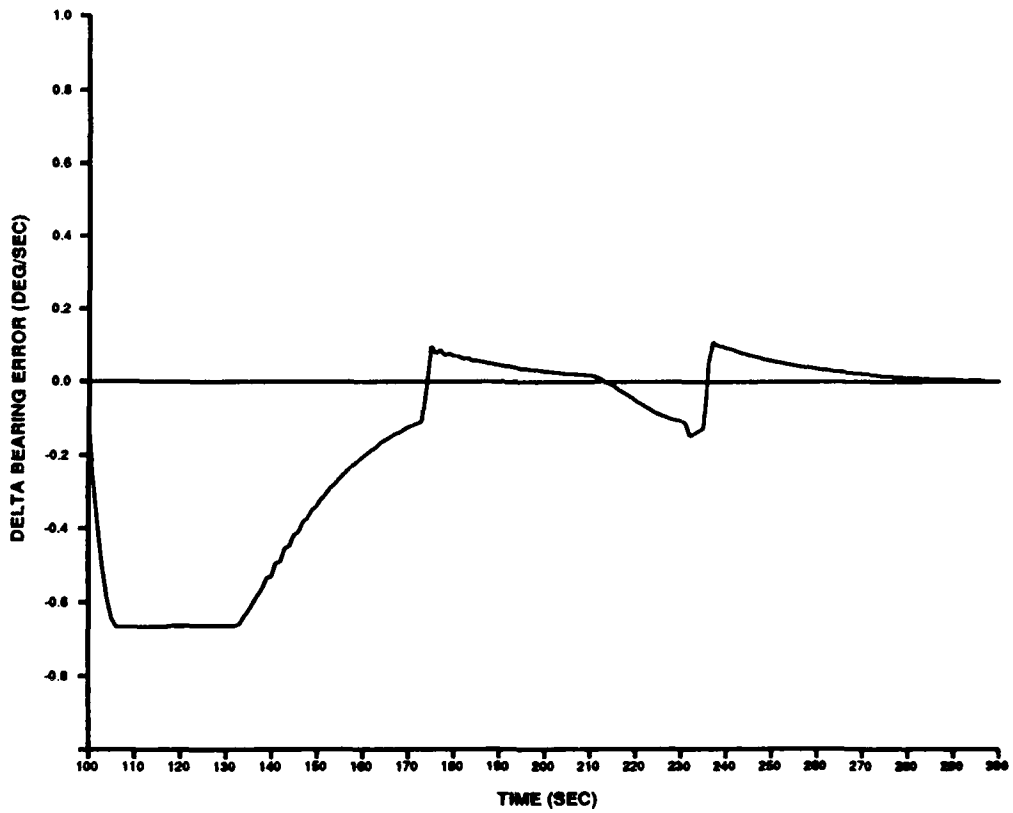


Figure 15b. Change in Error Between Vehicle and Contact Bearings for Run 4

At 174 seconds, which is prior to the maneuver, the vehicle has already crossed the contact bearing line. The reversal of the bearing line motion, caused by the maneuver, results in an increase in the vehicle closure rate on the bearing line exhibited by the transient behavior in x_2 between 210 and 235 seconds. At 235 seconds, the vehicle crosses back over the contact bearing line to achieve the steady-state orientation for the new geometry. After 235 seconds, x_2 exhibits the same type of gradual decay as is seen in run 2 after 174 seconds. Thus, the evasive maneuver results in a transient in x_2 that is only a reflection of the change in the vehicle closure rate on the contact bearing line; the radical maneuver does not produce any radical perturbations in the guidance point bearing error, x_1 . The trajectory plot for run 4 is given in figure 15c.

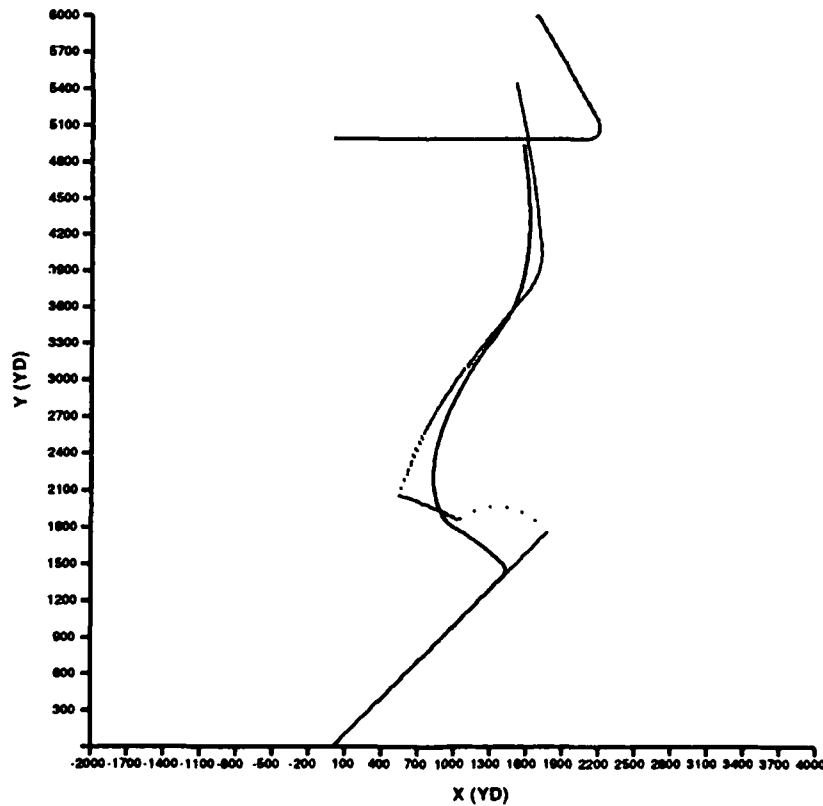


Figure 15c. Fuzzy Beam Rider Trajectory for Run 4

Run 5 is similar to run 4; the difference being that at 210 seconds, the contact maneuvers to a course of 120°. This produces a situation in which the contact is closing in range on the vehicle as opposed to run 4 where the maneuver produces an opening geometry. Figures 16a and 16b are identical to figures 15a and 15b up to 210 seconds, as should be the case. In figure 16b, the same type of decay is observed for x_2 after 174 seconds until the contact maneuvers at 210 seconds. The maneuver for this case produces a larger positive increase in the contact bearing rate. The only effect is a minor transient condition at 210 seconds that results in a rapid increase in x_2 to a higher value, reflecting the decrease in vehicle closure rate. Because the maneuver does not require the vehicle to cross the bearing line to attain the new steady-state orientation, steady state for the new geometry is quickly attained (approximately 7 seconds after the maneuver) and x_2 decreases in a similar fashion as before. As was the case in run 4, this evasive maneuver had little effect on system performance. The trajectory plot for run 5 is given in figure 16c.

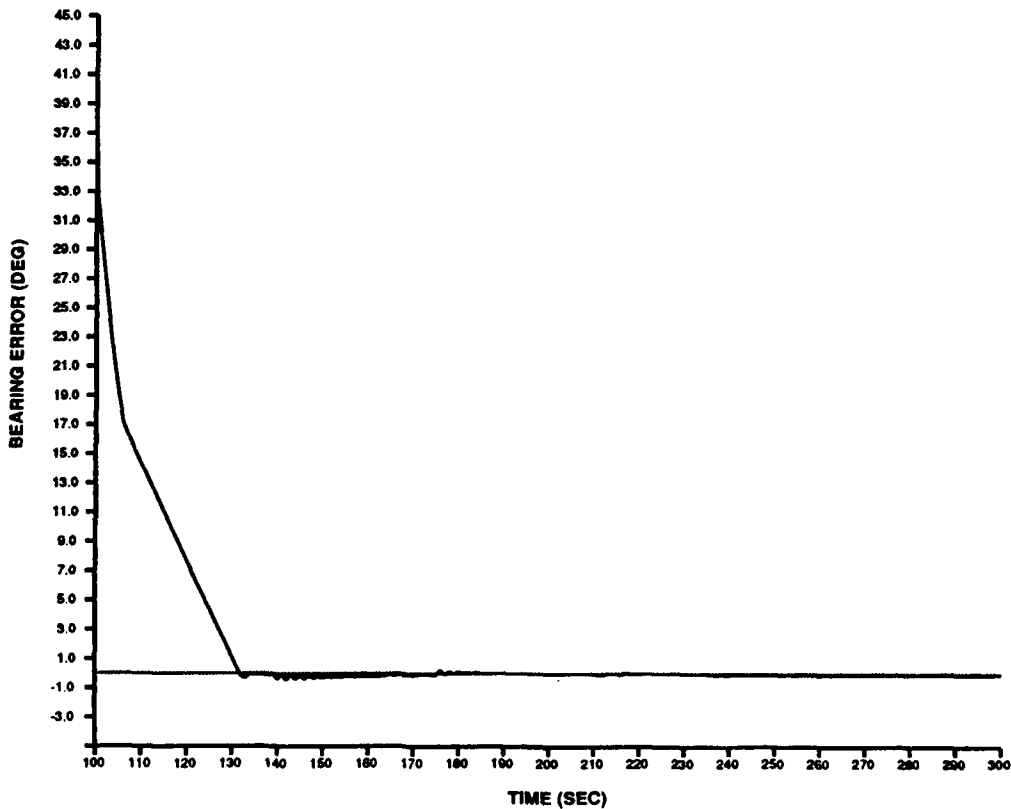


Figure 16a. Guidance Point Bearing Error for Run 5

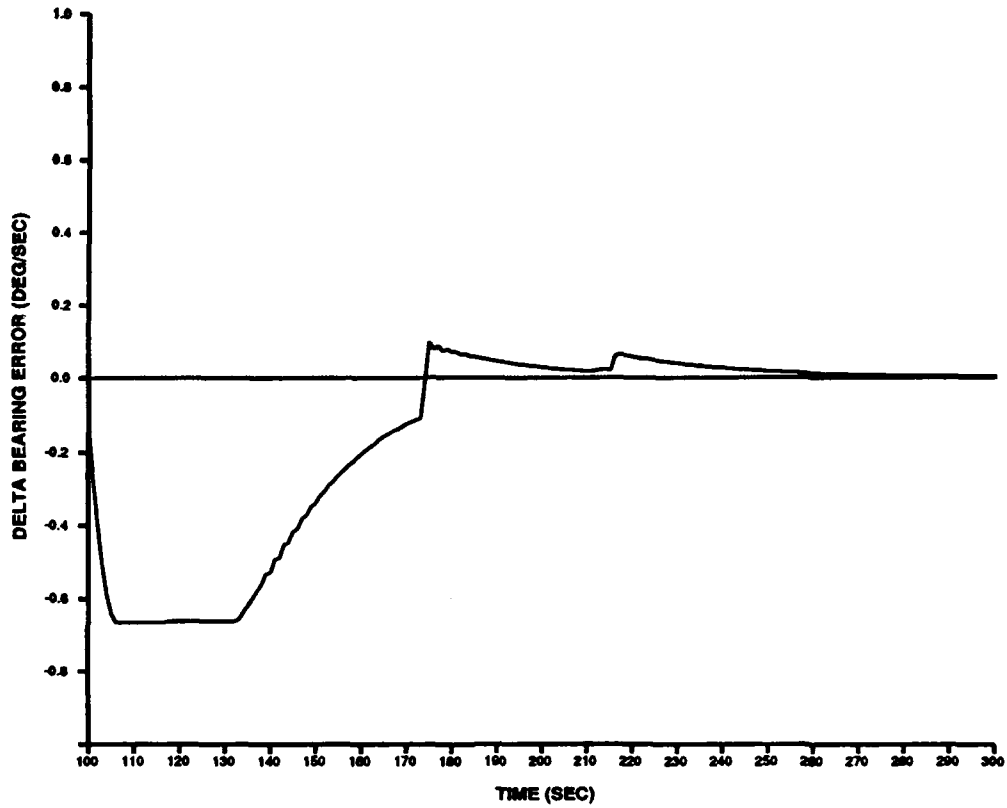


Figure 16b. Change in Error Between Vehicle and Contact Bearings for Run 5

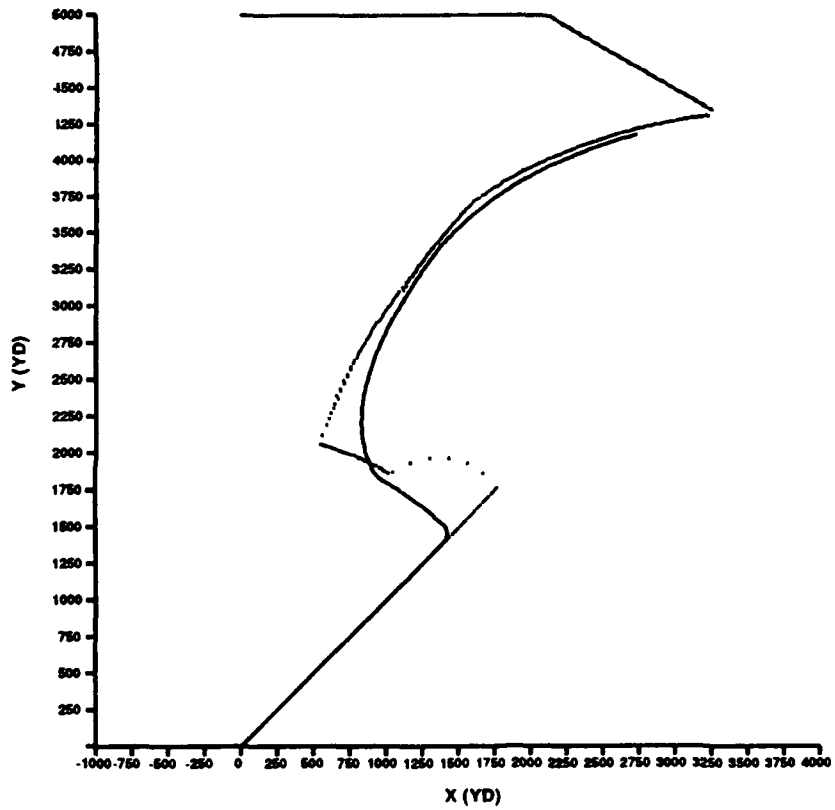


Figure 16c. Fuzzy Beam Rider Trajectory for Run 5

While the contact maneuvers in runs 4 and 5 occur after the vehicle has reached steady state, the remaining two runs demonstrate behavior when the contact maneuvers occur prior to steady state. In run 6 (figures 17a, 17b, and 17c), the same type of evasion as in run 4 is examined except the maneuver takes place earlier at 125 seconds, prior to the vehicle laminar point's first crossing of the contact bearing line. Comparing figures 13a and 17a, it is seen that the maneuver appears to slightly enhance system performance, i.e., steady operation is attained earlier (at about 141 seconds versus 151 seconds). This slight improvement is due to the maneuver resulting in a steady-state geometry that does not require the vehicle to cross the contact bearing line.

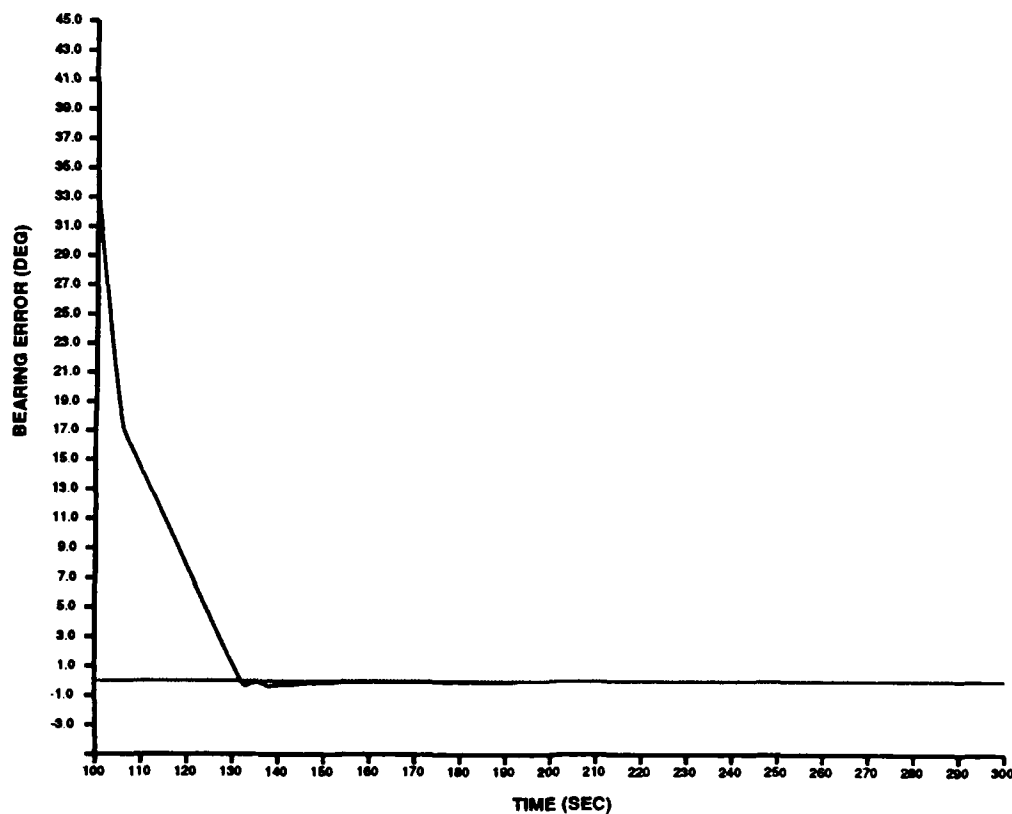


Figure 17a. Guidance Point Bearing Error for Run 6

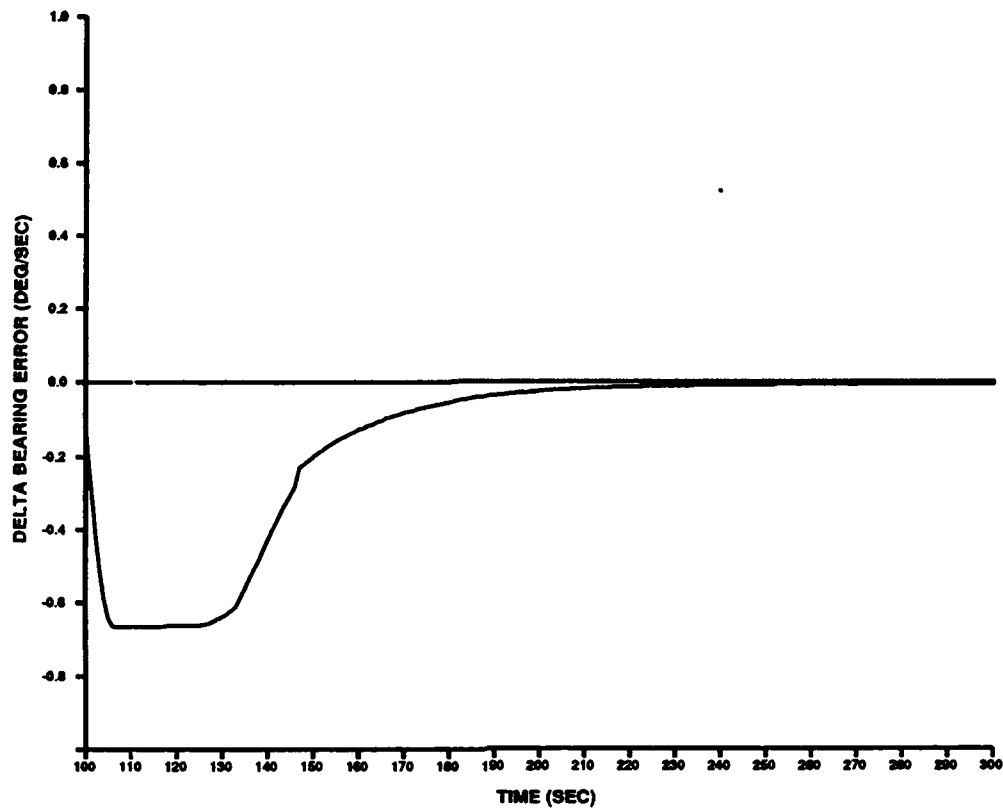


Figure 17b. Change in Error Between Vehicle and Contact Bearings for Run 6

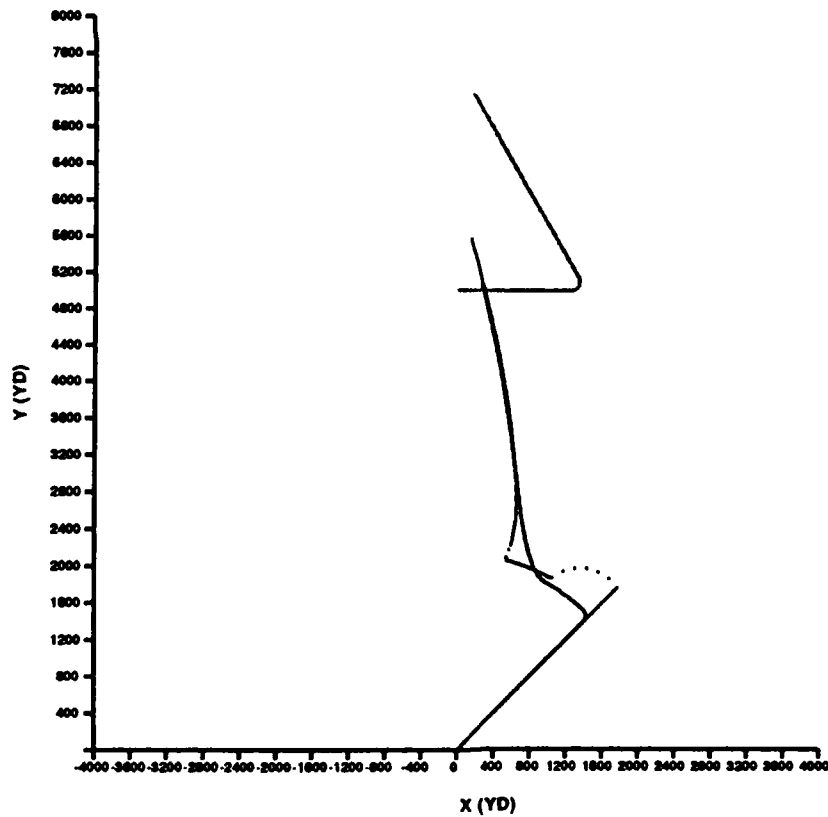


Figure 17c. Fuzzy Beam Rider Trajectory for Run 6

In run 7 (figures 18a, 18b, and 18c), the contact again evades at 125 seconds but performs the same maneuver as in run 5. Again, system performance is not greatly affected by the evasive maneuver. The only difference is the increased closure rate (figure 18b) caused by the maneuver that allows the vehicle to cross the contact bearing line earlier (166 seconds versus 174 seconds) to attain a steady-state orientation for the new geometry. Once in the steady-state geometry, x_2 exhibits the same type of decay as was seen in previous runs.

The trajectory plots for runs 4, 5, 6, and 7 have been given in figures 15c, 16c, 17c, and 18c. As in the previous stationary and linear contact motion cases, good control behavior is exhibited for vehicle bearing rider operation in all the nonlinear runs. The type or time of the contact maneuvers does not require the vehicle to undergo any radical trajectory changes to compensate for contact evasive behavior.

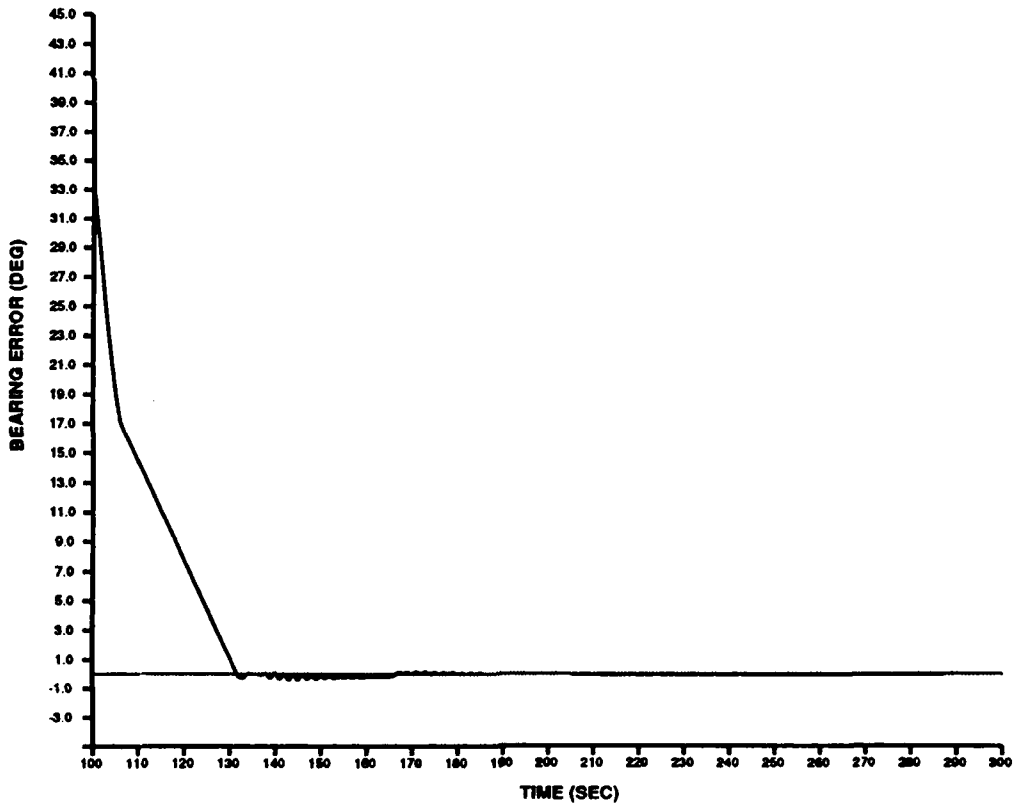


Figure 18a. Guidance Point Bearing Error for Run 7

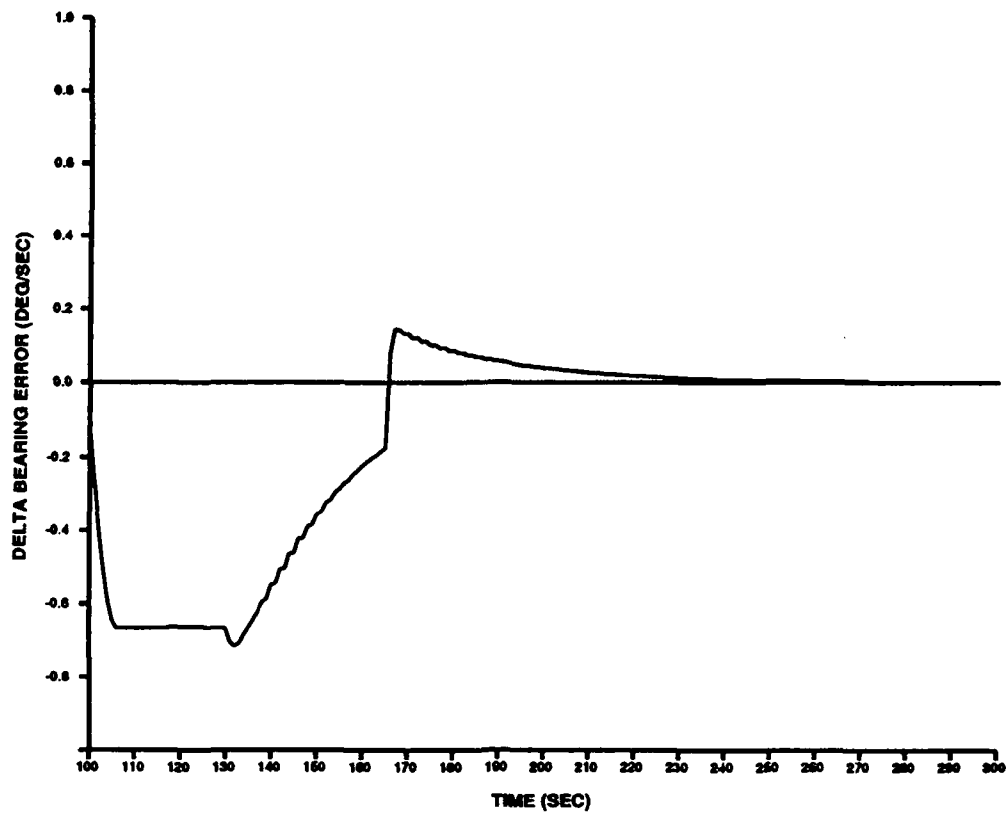


Figure 18b. Change in Error Between Vehicle and Contact Bearings for Run 7

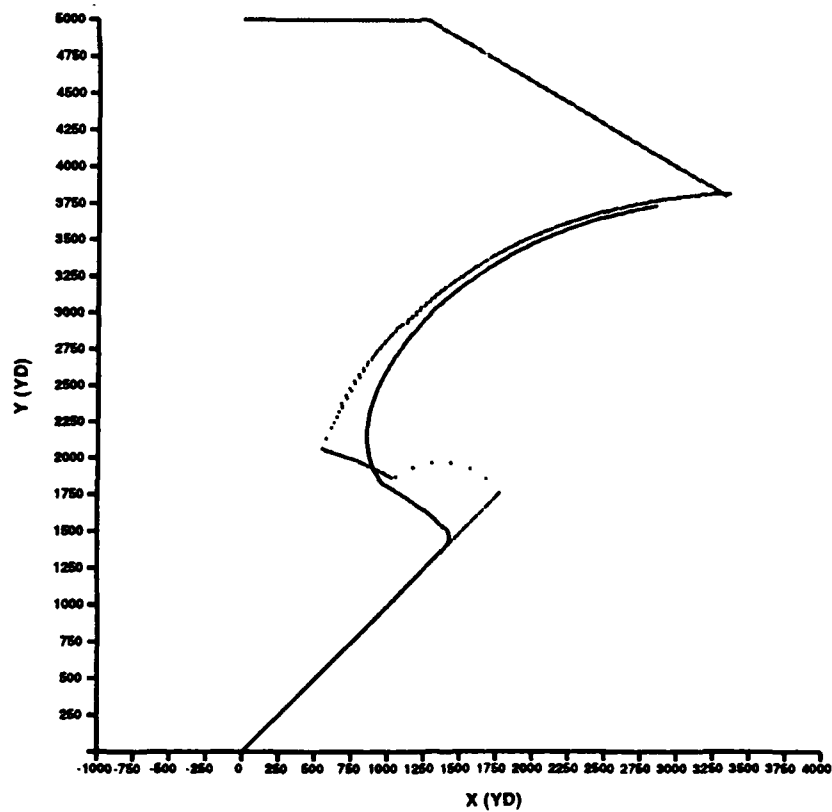


Figure 18c. Fuzzy Beam Rider Trajectory for Run 7

CONCLUSIONS

A fuzzy control system for beam rider guidance of a vehicle launched from a moving platform against an evasive contact was formulated. Robust performance was demonstrated via the use of a computer simulation.

Beam rider control required the determination of vehicle commands that placed/maintained a point, a fixed distance ahead of the vehicle, on or near a time-varying contact bearing line. It should be noted that the change in the position of the guidance point due to a given course command is proportional to the selected distance. Selection of this distance in tactical applications is a function of many parameters.

Good system performance was achieved by the fuzzy controller by using two sets of rules. Each set of rules used indications of the size of the angular errors between the contact and vehicle laminar point bearings in conjunction with a 1-second estimate of the vehicle's closure/opening rate on the bearing line. A different set of rules was required, depending on what side of the contact bearing line the vehicle was on. The rules were formulated by using only intuitive knowledge and experience regarding characteristic beam rider operation. Formulation of the controller did not require any further mathematical description of system dynamics. Commands generated by the controller produced smooth vehicle trajectories, during both transient and steady state, for all runs examined. The guidance point was placed in the proximity of the bearing line as rapidly as possible (given the constraint imposed because of tactical considerations) with minimum overshoot and maintained on/near the line for various types of contact motion (stationary, linear, and nonlinear behavior).

The constrained fuzzy beam rider guidance scheme that has been devised has the following advantages and new features:

- The fuzzy controller design emulates operations that reflect heuristic considerations through the use of a rule-based expert system in which is embedded a knowledge base that reflects the thinking processes a human might go through in manipulating the system.
- The controller command constraints are based on the latest tactical situation information.
- The fuzzy controller design automatically generates and issues vehicle control commands such that the vehicle follows a beam rider trajectory.
- The fuzzy control scheme is a simple design that provides robust behavior. As new situations arise, the controller design has the inherent capability to be tuned by using experimental data from the new situations.

Further studies are continuing in the design of fuzzy postlaunch vehicle controllers. One area is concerned with an adaptive mechanism that ensures robust behavior as vehicle tactical parameters are changed.

REFERENCES

1. B. Kosko, *Neural Networks and Fuzzy Systems*, Prentice-Hall, Englewood Cliffs, NJ, 1992.
2. C. C. Lee, "Fuzzy Logic in Control Systems: Fuzzy Logic Controller Part I and Part II," *IEEE Transactions on Systems, Man, and Cybernetics*, vol. 20, no. 2, pp. 404-435, March/April 1990.
3. E. Cox, "Fuzzy Fundamentals," *IEEE Spectrum*, pp. 58-61, October 1992.

INITIAL DISTRIBUTION LIST

Addressee	No. of Copies
Commander, Submarine Force Atlantic Fleet	1
Commander, Submarine Force Pacific Fleet	1
Chief of Naval Operations (NOP-24, NOP-71, NOP-75, NOP-987)	4
Chief of Naval Research (OCNR-12, OCNR-23)	2
Space and Naval Warfare Systems Command (PD-80)	1
Naval Sea Systems Command (SEA-06U, SEA-06V, SEA-63, PMO-425 -- R. Dosti)	4
Naval Postgraduate School	1
Naval War College	1
Submarine Training Facility, Atlantic	1
Submarine Training Facility, Pacific	1
Defense Technical Information Center	2
Center for Naval Analyses	1